On Using Storage and Genset for Mitigating Power Grid Failures

by

Sahil Singla

A thesis
presented to the University of Waterloo
in fulfillment of the
thesis requirement for the degree of
Master of Mathematics
in
Computer Science

Waterloo, Ontario, Canada, 2013

© Sahil Singla 2013

I hereby declare that I am the sole author of this thesis. This is a true copy of the thesis, including any required final revisions, as accepted by my examiners.

I understand that my thesis may be made electronically available to the public.

Abstract

Although modern society is critically reliant on power grids, even modern power grids are subject to unavoidable outages due to storms, lightning strikes, and equipment failures. The situation in developing countries is even worse, with frequent load shedding lasting several hours a day due to unreliable generation.

We study the use of battery storage to allow a set of homes in a single residential neighbourhood to avoid power outages. Due to the high cost of storage, our goal is to choose the smallest battery size such that, with high target probability, there is no loss of power despite a grid outage. Recognizing that the most common approach today for mitigating outages is to use a diesel generator (genset), we study the related problem of minimizing the carbon footprint of genset operation.

Drawing on recent results, we model both problems as buffer sizing problems that can be addressed using stochastic network calculus. We show that this approach greatly improves battery sizing in contrast to prior approaches. Specifically, a numerical study shows that, for a neighbourhood of 100 homes, our approach computes a battery size, which is less than 10% more than the minimum possible size necessary to satisfy a one day in ten years loss probability $(2.7 * 10^4)$. Moreover, we are able to estimate the carbon footprint reduction, compared to an exact numerical analysis, within a factor of 1.7.

We also study the genset scheduling problem when the rate of genset fuel consumption is given by an affine function instead of a linear function of the current power. We give alternate scheduling, an online scheduling strategy that has a competitive ratio of $\frac{k_1 \frac{G}{C} + k_2}{k_1 + k_2}$, where G is the genset capacity, C is the battery charging rate, and k_1, k_2 are the affine function constants. Numerically, we show that for a real industrial load alternate scheduling is very close to the offline optimal strategy.

Acknowledgements

I am grateful to my supervisor, Professor S. Keshav, for his invaluable support, guidance, and feedback for my thesis. I would like to thank Y. Ghiassi-Farrokhfal, and other members of the ISS4E lab, who collaborated with me on various projects. I am also thankful Professor Johnny Wong and Professor Catherine Rosenberg to be the readers of this thesis and providing their useful feedback.

Dedication

This thesis is dedicated to my family– my parents, who have been always supportive, and my younger sister, who has been always critical :-)

Table of Contents

List of Figures

Chapter 1

Introduction

The power grid underlies most modern societies: power failures can affect critical institutions such as hospitals, water treatment facilities, aircraft control towers, and Internet data centres. Despite this great reliance on electrical power, as the aftermath of super-storm Sandy vividly demonstrated, even modern power grids are subject to unavoidable outages due to storms, lightning strikes, and equipment failures. The situation in developing countries is worse, with daily load shedding lasting two-to-four hours due to demand spikes and unreliable generation [31]. India recently suffered world's largest blackout leaving more than 600 million people without power [21]. In the face of this inherent unreliability, the standard solution is for critical facilities, and even some individual homes, to augment grid power with local generation, typically from a diesel generator. This, however, inherently increases the carbon footprint of the load [28].

Using a two-way inverter to convert between AC and DC power, batteries can store power when the electricity from the grid is available and discharge to meet the load during a time of power outage. Advances in electric vehicle energy storage technology have led to a sustained decrease in the price of electrical storage [32]. This motivates us to study, in Chapter 3, the use of battery storage to allow a set of homes in a single residential neighbourhood to avoid power outages. In essence, the entire neighbourhood can be thought to be connected to a single large uninterruptible power supply.

Storage is still expensive, however, so our goal is to choose the smallest battery size such that, with high target probability, there is no loss of load despite a grid outage. Recognizing that the most common approach today for mitigating outages is to use diesel generators, we also

study the related problem of minimizing the carbon footprint of diesel generator operation by minimizing generator operation .

The efficiency of a genset to consume fuel and produce energy is known to be maximum when it operates close to its capacity. In Chapter 4, we go deeper into genset modeling and study how storage can be used to improve genset efficiency of a remote industry not connected to the power grid. A battery helps in reducing fuel consumption by meeting low demands itself and turning OFF the genset. The battery is recharged whenever the genset is turned ON. Scheduling of power between the battery and the genset is no longer trivial and we give an online scheduling strategy with performance close to the offline optimal strategy. A battery-genset hybrid system can meet demand simultaneously using the genset and the battery. A battery can therefore also help in decreasing total fuel consumption by preventing over-sizing of the genset. Hence, we use techniques from stochastic network calculus to address the problem of sizing genset and the battery while ensuring that the loss of load probability is below a threshold.

Chapter 2

Background and Preliminaries

The problem of battery sizing in power distribution systems can be mapped to the problem of buffer sizing in the teletraffic network. This analogy has been used in some recent papers for battery sizing, borrowing state-of-the-art analytical results on probabilistic buffer sizing from teletraffic theory [2, 39, 41]. We briefly discuss the essence of this analogy in this section.

2.1 Deterministic loss of power vs. deterministic loss of packet

Suppose that an arrival process A enters a buffer (queue), which can serve traffic at rate C, and let A' be the corresponding departure process. We assume discrete time model, where the events can only happen at discrete time instants, i.e., $t = 0, 1, \ldots$. We denote the total arrival from process A in time interval $[0, t]$ by $A(t)$ and we use $A(s, t)$ to mean $A(t) - A(s)$. The *backlog* $b(t)$ at any time t is defined to be the buffer content at that time. If the buffer size is infinite then the backlog at any given time is simply the difference between A and A', i.e.

$$b(t) = A(t) - A'(t) .$$

This formulation, however, will no longer hold if the buffer size B is finite. Instead, it can be obtained from the following recursive equation:

$$b(t) = \min(B, [b(t-1) + A(t-1, t) - C]_+) , \tag{2.1}$$

where $[x]_+ = \max(0, x)$ for any value of x. Cruz and Liu [13] transformed this recursion into the following non-recursive expression:

$$b(t) = \min_{0 \leq u \leq t} \left(\max_{u \leq s \leq t} \left(A(s, t) - C.(t - s), \right.\right.$$
$$\left.\left. A(u, t) - C.(t - u) + B \right) \right). \tag{2.2}$$

The loss of traffic due to buffer overflow at time t is

$$l(t) = [A(t - 1, t) - C + b(t - 1) - B]_+ . \tag{2.3}$$

Eqs. (2.2-2.3) can be combined to extract the following loss characterization [13]:

$$l(t) = \min_{0 \leq u \leq t-1} \left(\max_{u \leq s \leq t-1} \left([A(s, t) - C.(t - s) - k(t)]_+, \right.\right.$$
$$\left.\left. [A(u, t) - C.(t - u) + k(u) - k(t)]_+ \right) \right), \tag{2.4}$$

where

$$k(t) = \begin{cases} B & t > 0 \\ 0 & t = 0 \end{cases} \tag{2.5}$$

A buffer sizing scheme must ensure that the amount of loss is kept below a certain threshold.

An analogous problem in the power system arises for the following scenario. A source with constant power C is feeding a battery and the battery output process is used to serve an intermittent demand. The *loss of power* event is defined as the event that a demand finds the battery empty. It can be easily seen that this problem is similar to the queuing problem in a finite buffer system with fixed capacity link and varying arrival process except that the direction of the input and output processes are the opposite in these two scenarios. The last piece of this mapping is the concept of the *deficit battery status* $b^d(t)$, which indicates the amount of energy needed at time t to fully charge the battery and can be computed recursively from the following:

$$b^d(t) = \min(B, [b^d(t - 1) + D(t - 1, t) - C]_+), \tag{2.6}$$

where $D(t - 1, t)$ is the demand at time slot t. Comparing Eq. (2.1) and Eq. (2.6) suggests that the mapping between the teletraffic queue analysis and power distribution battery analysis when the deficit battery charge is mapped to the backlog status, the demand D is mapped to the arrival

traffic A, and the power supply is mapped to the capacity (service rate) of the link [2, 40]. This mapping can also be verified intuitively by seeing that the two problems are analogous if the direction of the input and output are reversed. Similarly, the buffer content is mapped to the compliment of the battery state of charge, which is the deficit state of charge.

To complete the picture, the loss of power at time t (the event that there is a demand and the battery is depleted and cannot serve it) is equal to $[b^d(t-1) - C + D(t-1, t) - B]_+$, which can be obtained from Eq. (2.3). Thus, the non-recursive equations for the backlog and loss in a finite buffer system in Eqs. (2.2) and (2.4) can be employed with the previously mentioned mapping to compute the loss of power probability in power distribution systems.

2.2 Probabilistic loss formulations

A buffer (battery) sizing approach requires an upper bound on the loss probability based on the statistical properties of the arrival (demand) and the link capacity (power source). The probabilistic loss formulation has been studied extensively in the asymptotic regime when the number of independent arrivals is large (*many sources asymptotic regime*)[15]. Since the battery allocation in the distribution systems does not have many allocated power sources and they are not independent, the results corresponding to the many sources asymptotic regimes cannot be used in this context. However, there are other alternatives that can be used in this context. We review the alternatives next.

Special case of regulated traffic

Kesidis and Konstantopoulos [24] provide a non-asymptotic upper bound on the loss probability for a so-called *peak-rate constrained leaky-bucket* process, which is a regulated arrival process A satisfying:

$$\forall s, t: \quad A(s, t) \leq \min(\pi(t - s), \sigma + \rho(t - s)) \tag{2.7}$$

for some π, σ and ρ such that $\rho \leq \pi$. If a *stationary* peak-rate constrained leaky-bucket arrival process is fed to a link with total capacity C, where $\rho \leq C \leq \pi$, then the stationary backlog

status b satisfies the following overflow probability:

$$\Pr\{b > B\} \leq \frac{\sigma - \frac{\pi - \rho}{\pi - C}B}{\frac{C}{\rho}\sigma - B} \, . \tag{2.8}$$

This formulation is used in [3] to compute transformer/storage sizing in the distribution networks.

General arrival using Network Calculus

Network Calculus allows probabilistic performance analysis including loss probability for a large class of arrivals. This theory uses upper bounds on the arrivals and lower bounds on the available service on different time scales to compute performance bounds. We only elaborate on a few concepts of this theory, which we use in this paper. Interested readers can refer to [5, 10, 20] for more complete discussions.

There are different probabilistic upper bounds in the literature, which can be used for performance analysis. For a complete survey on the existing envelopes in the literature please refer to [29]. Here we use a concept called the *statistical sample path envelope* [8]. A non-decreasing function $\mathcal{G}$ is a statistical sample path envelope for an arrival process A with bounding function ε if it satisfies the following for any time $t \geq 0$ and any $\sigma \geq 0$

$$\Pr\left\{\sup_{s \leq t}\{A(s,t) - \mathcal{G}(t-s)\} > \sigma\right\} \leq \varepsilon(\sigma) \, , \tag{2.9}$$

where $\varepsilon(\sigma)$ is non-increasing in σ.

The exact loss description from Eq. (2.4) is too complicated to be used directly for loss probability formulations. Hence, to extend the results to the probabilistic settings, the following upper bound on Eq. (2.4) is used in [13]

$$l(t) \leq \max_{0 \leq s \leq t}\left([A(s,t) - C.(t-s) - B]_+\right) \, . \tag{2.10}$$

This upper bound on the loss at time t is used in the following theorem to derive an upper bound on the loss of power probability.

Theorem 1 (Loss of power probability [39]). *Suppose that $\mathcal{G}$ is the statistical sample path envelope for a demand process D in the sense of Eq. (2.9) with bounding functions ε_g. Then, the loss*

6

of power probability satisfies the following:

$$\Pr\{l(t) > 0\} \leq \varepsilon_g \left(B - \sup_{0 \leq \tau \leq t} \left(\mathcal{G}(\tau) - C\tau \right) \right). \tag{2.11}$$

If there is a measurement trace of demands over time, the statistical sample path envelope $\mathcal{G}$ can be computed by (1) constructing sample values for the event $\{A(s,t) - \mathcal{G}(t-s)\}$ for each trajectory and any time t, and (2) use the complementary cumulative distribution function (CCDF) of the sample set as a bounding function for Eq. (2.9) [12].

Markovian arrival using Network Calculus

Sometimes an arrival model is given instead of a measurement set. One of the most general and widely-used models is the multi-state Markovian (MSM) fluid flow process, which is a Markov chain with finite states, with states representing the rate at which traffic is generated at a certain time. Theorem 1 can be used to obtain a loss probability for MSM processes since there is a statistical sample path envelope for this type of processes, which can be computed as follows:

An M-state fluid flow Markov chain with transition matrix Q and traffic rate at state i being r_i satisfies the following: [22]

$$\forall t : \quad E\left[e^{\beta A(t)}\right] \leq e^{\rho(\beta)t}, \tag{2.12}$$

where $\rho(\beta)$ is the largest eigenvalue of the matrix $\frac{1}{\beta}Q + R$ and $R = diag(r_i)$. Combining Chernoff bound and Eq. (2.12) yields the following for any time t and s ($\leq t$) and any σ (≥ 0)

$$\Pr\{A(s,t) > \rho(t-s) + \sigma\} \leq e^{-\beta\sigma} \tag{2.13}$$

which shows that a multi-state Markovian process is a special case of the large class of exponentially bounded burstiness traffic sources (EBB) [42]. For such a traffic, $\mathcal{G}$ from the following is a statistical sample path envelope in the sense of Eq. (2.9) with bounding function ε for any $\gamma > 0$ and any σ (≥ 0) [11]

$$\mathcal{G}(t) = (\rho(\beta) + \gamma)t; \qquad \varepsilon(\sigma) = \frac{e^{-\beta\sigma}}{1 - e^{-\beta\gamma}} \tag{2.14}$$

This can be verified as follows

$$\Pr\left\{\sup_{s\leq t}\{A(s,t)-\mathcal{G}(t-s)\}>\sigma\right\}$$
$$\leq \sum_{s\leq t}\Pr\{A(s,t)>(\rho+\gamma)(t-s)+\sigma\}$$
$$\leq \sum_{0\leq\tau\leq t}e^{-\beta(\gamma\tau+\sigma)}$$
$$= \frac{e^{-\beta\sigma}}{1-e^{-\beta\gamma}} \tag{2.15}$$

where union bound is used in the second line. A new variable is defined in the third line $\tau = t-s$ and the last line uses Eq. (2.13).

One can insert the statistical sample path envelope for a multi-state Markovian model from Eq. (2.14) to Theorem 1 to obtain a loss of power probability for such a demand.

Chapter 3

Storage sizing for unreliable Grid

Given that household loads are stochastic [17], the battery sizing problem is non-trivial. Indeed, it has been shown to be isomorphic to the complex–but well-known–problem of choosing a buffer large enough to smooth the data being generated by a variable-bit-rate traffic source [2, 39]. Therefore, drawing on recent results, we approach the solutions to both problems using the powerful techniques of stochastic network calculus. Specifically, we use a statistical sample path envelope (discussed in Section 2.2) to stochastically bound the load from a set of homes. This allows us to compute battery size and expected carbon footprint of diesel generator operation.

We have numerically evaluated the accuracy of our algorithms using real traces of electrical loads collected over 12 months from 4500 homes in Ireland[1] [9]. Analysis shows that, given a target requirement of a power outage being upper bounded by one day in ten years (a loss probability $(2.7 * 10^{-4})$), our approach computes a battery sizing that is only about 10% more than the minimum battery required had the future load been exactly known. Moreover, we are able to estimate the carbon footprint reduction, compared to an exact numerical analysis, within a factor of 1.7.

The key contributions of our work are:

1. We use a stochastic network calculus approach to analytically compute the battery size necessary to meet a target loss of power probability for a stochastic electrical load connected to a highly *unreliable* power grid.

---

[1]Although loads in Ireland are not the same as loads in developing countries, our methodology can be applied to traces collected from any country

2. Given the availability of a diesel generator (genset), and for a given load characterization, we find the genset carbon emission as a function of the battery size, thus allowing us to compute the battery size needed to limit carbon emissions below a target threshold.

3. We use measured electricity consumption data from 4500 Irish homes to compare our battery size and carbon emission bounds to those computed (a) empirically, (b) from bounds obtained using teletraffic theory, and (c) using a multi-state fluid Markov model. We find that our bounds are very close to the empirical optimal and far better than the two other approaches.

The rest of the chapter is laid out as follows. Section 3.1 starts with a motivation for the problem along with the prior work. The model used to analyze battery sizing problem along with our assumptions is explained in Section 3.2. The bounds on minimum battery size, both in presence and absence of genset, are computed in Section 3.3. These bounds are heavily dependent on the accuracy of statistical sample path envelope on effective demand. Hence, in Section 3.4, we explain how to obtain a tight envelope for any given load dataset. We show the tightness of our bounds numerically on the Irish dataset in Section 3.5 by comparing them to the bound obtained had the future load been exactly known and the bounds from prior work. Finally, Section 3.6 concludes the paper with the limitations and future work.

3.1   Motivation and Related Work

The difficulty of choosing a battery size sufficient to meet a stochastic load when confronted with stochastic power outages is illustrated in Figure 3.1. In this figure, the X axis shows the duration of a power outage, that is, a time during which the grid does not supply power, and the Y axis shows the state of charge of a battery of size 1 MWh that charges itself when the grid is available and discharges during an outage. Each line (trajectory) in the figure represents a particular power outage incident; the Y intercept of the line is the initial state of charge when the outage started and the line ends when the power outage ends. Each trajectory was computed using real measured loads from the Irish dataset (details in Section 3.5).

Most trajectories in Figure 3.1 start with the battery nearly full. This indicates that the inter-outage interval (in this particular numerical evaluation) is long enough to allow the battery to nearly fully charge before the next outage begins. However, some outages start with the battery
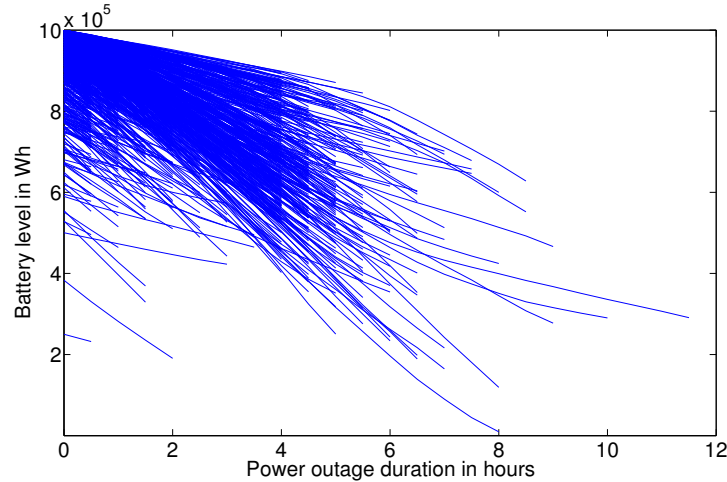
Figure 3.1: Trajectories of a battery of size $B = 10^6 Wh$ and charging rate $C = 10^5 W$ during power outage periods

state of charge as low as 250 kWh. This arises due to the combination of a long outage period followed immediately by a short inter-outage period.

We have a *loss of power* when the battery level drops to 0, a situation that we would very much like to avoid. In this numerical evaluation, the loss of power state happens only once. Note that had the battery size been somewhat smaller, say 400 KWh, we would have had a much larger number of loss of power events.

It is clear that the probability of a loss of power depends on many factors, including the battery size, its charging rate, a characterization of the load during a loss of power event, the distribution of the inter-outage intervals, and the distribution of outage durations. Moreover, what we seek to compute is the tail probability of the state-of-charge distribution of the battery. This is an inherently complex problem. However, it has recently been shown that this storage sizing problem is very similar to the buffer-sizing problem in a telecommunications network. We are inspired by new theoretical results in [39, 3], which adopt a queuing-theoretic buffer-sizing analysis to size batteries, to use a similar approach, based on stochastic network calculus, to study the problem of diesel and battery sizing for unreliable grids.

Specifically, we consider two scenarios. In the first scenario, we study a system that has only battery storage. Here, our goal is to find the minimum required battery size that meets a given

target loss of power probability, such as one day loss of power in every ten years. In the second (hybrid) system, we augment a battery with a genset. In this system, a loss of power will not occur because the diesel generator steps in when the battery is fully discharged. However, we still seek to size the battery so that the carbon discharge from the diesel generator is upper-bounded.

Prior work in this area relies primarily on empirical numerical analysis rather than analytical modeling [4, 34, 14]. Carbon emission due to a diesel-battery hybrid system has been studied mainly through the notion of genset efficiency, which is the diesel consumption per unit energy production [4, 30]. We note that some of the prior analytical works (e.g. [3]) assume load stationarity . In contrast, our approach does not need to explicitly assume stationarity.

A probabilistic loss of power formulation is presented in [39] for an intermittent power resource serving a stochastic demand with the aid of batteries. For a target loss of power probability, that formulation can be used for battery sizing. We point out that although there are similarities with our work, there are major differences between the system model in our problem and the one in [39]:

1. In the system model used in [39], the energy from the grid is fed to the battery and is not used to serve the energy demand directly. On the contrary, in our model, once available, the utility grid is used to serve the energy demand directly.

2. We assume a utility grid with infinite power supply with random off periods, while a finite power renewable energy is assumed in [39].

In essence, [39] considers battery sizing for intermittent resources (e.g., wind and power) to serve an intermittent demand. In the problem studied there, it is possible for the grid to be available yet not be sufficient to serve the instantaneous demand of both charging the battery and serving the demand. In our system, however, if the energy supply from the grid is available then it is assumed to be large enough to serve both the instantaneous demand and charge the battery at its maximum charging rate C.

3.2 System Model

The system model considered in this paper is illustrated in Figure 4.2. The grid and a battery are used to serve the demand. The grid is available irregularly. If the grid is available, then it is

12

used to serve the demand and charge the battery. When the grid is not available, the charge of the battery is used to serve the demand. Denote by $d(t)$ the energy demand at time slot t, and by $D(t)$ the cumulative energy demand in time interval $[0, t]^2$. To simplify notation, we define $D(s, t) = D(t) - D(s)$. The charging rate of the battery is represented by C and the battery size by B. We assume a discrete time model, where $t = 0, 1, \ldots$. Let $x(t)$ be a binary random variable representing the availability of the utility grid at time slot t, *i.e.*,

$$x(t) = \begin{cases} 0 & \text{If the grid is unavailable (outage) at time slot } t \\ 1 & \text{If the grid is available at time slot } t \end{cases} \tag{3.1}$$

We define $x^c(t) = 1 - x(t)$ as the complement of $x(t)$. If the grid is available in time slot t (i.e., $x(t) = 1$), the energy demand is served by the grid and the battery will be charged by as much as C energy unit in that time slot. On the other hand, if the grid is not available (i.e., $x(t) = 0$), the energy demand must be served by the energy stored in the battery.

We follow two objective functions for battery sizing in this paper. First, in the absence of genset, we size the battery B such that given some statistical properties of the energy demand process, the probability of loss of power is kept below a target threshold ϵ^*. Second, in the presence of genset, we size the battery such that the total carbon footprint is kept below a certain threshold.

We have the following assumptions in our formulations

1. Battery charging rate is upper bounded by C but there is no constraint on the discharge rate. [3]

2. Genset is large enough to meet the maximum aggregate loads.

The above assumptions typically hold in practice since battery charge rate depends on the technology of the battery, and for technologies such as lead-acid battery, the discharge rate is around five times higher than the charging rate [6]. Moreover, the marginal cost of increasing genset size is negligible compared to the marginal cost of a battery [35, 38].

---

[2]The energy demand varies widely over the course of a year showing marked seasonality. Our analysis is agnostic to the time interval over which the demand is modeled. In practice, however, similar to the concept of busy-hour sizing in a telecommunication network, we advocate the sizing of a battery keeping in mind the underlying non-stationarity of the demand process [3].

[3]Note that a constant battery charge-discharge energy loss factor can be incorporated in C as it would just reduce the original battery charging rate by this factor.

Name	Description
Outage	Electricity from the grid is unavailable
Loss of power	An outage period with battery being empty
B	Battery storage capacity
C	Battery charging rate
ϵ^*	Target loss of power probability
$x(t)$	Grid availability at time t
$x^c(t)$	Grid unavailability at time t
$d(t)$	Power load at time t
$d^e(t)$	Effective power load to battery at time t
$b(t)$	Battery energy level at time t
$b^d(t)$	Battery deficit energy level at time t
$l(t)$	Loss of power at time t
$\mathcal{G}$	Statistical sample path envelope
ε_g	Bounding function for sample path envelope

Table 3.1: Notation

3.3   Battery Sizing Formulation

The unreliable grid described in our problem statement can be converted to a reliable *compound* power source i.e., one that is augmented by batteries. In this section we compute the required battery size such that a target loss probability can be guaranteed for the combination of the unreliable grid and the battery size. The size of the battery is a function of how frequent and for how long the grid is unavailable.

3.3.1   Loss of power Formulation

As discussed in Section 3.1, there are major differences between our problem system model and the one assumed in [39] that do not allow using the loss of power formulation for our problem directly. However, we use a clever substitution to let us use the results in [39] in our work.

(a) Grid available

(b) Power Outage
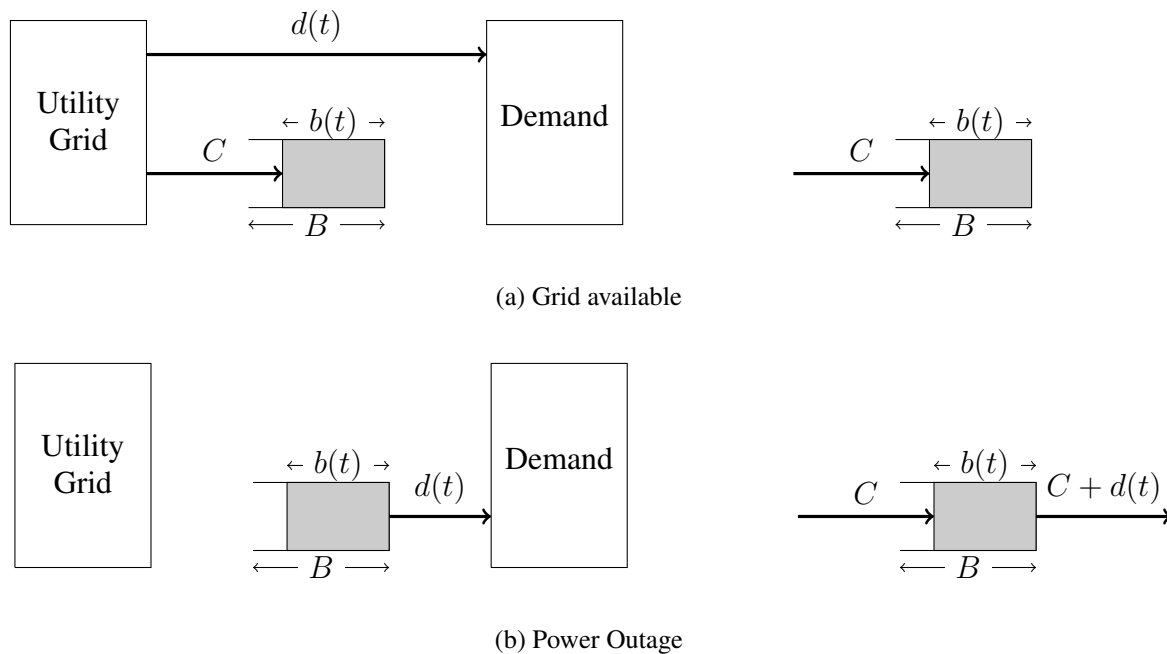
Figure 3.2: Battery storage model before and after transformation

Consider the input and output processes to the battery separately for the cases where the grid is available ($x(t) = 1$) and unavailable ($x(t) = 0$). If $x(t) = 1$, the arrival energy process to the battery at any time instant t is a constant, C, and the departure energy process is zero. If $x(t) = 0$, the arrival energy process is zero and the departure energy process is $d(t)$. The battery state-of-charge does not change if we assume that the real arrivals and departures to the battery are both shifted by the same constant at any time. Therefore, we can assume C and $d(t) + C$, respectively, as the arrival and departure processes when $x(t) = 0$ (instead of 0 and $d(t)$) and have the same battery state of charge (see Figure 4.2). Combining the two cases $x(t) = 0$ and $x(t) = 1$ with the above substitution, we can assume that the battery is always charged with rate C and discharged by the *effective demand* d^e defined as:

$$d^e(t) = [d(t) + C](1 - x(t))$$
$$= [d(t) + C]x^c(t) \tag{3.2}$$

which is the portion of the demand that the battery must serve. Using the above transformation

15

and from Eq. (2.6), we have:

$$b^d(t) = \min(B, [b^d(t-1) + d^e(t) - C]_+) \,. \tag{3.3}$$

With the above mapping, the loss formulation in the previously mentioned finite buffer system is given by $l(t) = [b^d(t-1) + d^e(t) - C - B]_+$. Hence, we can use Eq. (2.4) to describe the following loss process as follows:

$$l(t) = \min_{0 \le u \le t-1} \left(\max_{u \le s \le t-1} \left([D^e(s,t) - C.(t-s) - k(t)]_+, \right.\right.$$

$$\left.\left. [D^e(u,t) - C.(t-u) + k(u) - k(t))]_+ \right) \,, \right. \tag{3.4}$$

where D^e is the cumulative version of the effective demand (Eq. (3.2)) and k is as expressed in Eq. (2.5).

3.3.2 Battery Sizing in the absence of genset

The exact loss description from Eq. (3.4) is difficult to use in practice. Instead, we use the following upper bound (from [18]) to derive an upper bound on the loss probability:

$$l(t) \le \min \left([d^e(t) - C]_+, \max_{0 \le s \le t-1} \left([D^e(s,t) - C(t-s) - B]_+ \right) \right) \tag{3.5}$$

$$= \min \left(d(t)x^c(t), \max_{0 \le s \le t-1} \left([D^e(s,t) - C(t-s) - B]_+ \right) \right) , \tag{3.6}$$

where in Eq. (3.5) we pick two specific values for u in the minimization of Eq. (3.4): $u = t - 1$ and $u = 0$. Eq. (3.6) uses the definition of $d^e(t)$ and that $d(t) > 0$. The above inequality can be used to compute a probabilistic upper bound on the loss probability for our problem.

Theorem 2. *Suppose that an unreliable grid uses a battery of size B with charging rate C to serve a demand. Suppose also that $x^c(t)$ represents the grid unavailability at time slot t ($x^c(t) = 1$ if the grid is unavailable and $x^c(t) = 0$, otherwise) and $\mathcal{G}$ is a statistical sample envelope for process D^e with bounding functions ε_g in the sense of Eq. (2.9). Then, the loss of*

16

power probability satisfies the following

$$\Pr\{l(t) > 0\} \leq \min\Bigg(\Pr\{x^c(t) > 0\},$$

$$\varepsilon_g \left(B - \sup_{\tau \geq 0}(\mathcal{G}(\tau) - C\tau) \right) \Bigg). \tag{3.7}$$

Proof. The loss probability at any time t satisfies the following

$$\Pr\{l(t) > 0\}$$

$$\leq \Pr\Bigg\{ \min\Bigg(d(t)x^c(t),$$

$$\max_{u \leq s \leq t-1} \left([D^e(s,t) - C(t-s) - B]_+ \right) \Bigg) > 0 \Bigg\} \tag{3.8}$$

$$\leq \min\Bigg(\Pr\{d(t)x^c(t) > 0\},$$

$$\Pr\Bigg\{ \max_{0 \leq s \leq t-1}(D^e(s,t) - C(t-s) - B) > 0 \Bigg\} \Bigg) \tag{3.9}$$

$$\leq \min\Bigg(\Pr\{x^c(t) > 0\}, \varepsilon_g \left(B - \sup_{\tau \geq 0}(\mathcal{G}(\tau) - C\tau) \right) \Bigg) \tag{3.10}$$

where we use Eq. (3.6) to derive Eq. (3.8). Eq. (3.9) is an upper bound on Eq. (3.8) using the fact that $P(X \cap Y) \leq \min(P(X), P(Y))$ for any events X and Y. Eq. (3.10) uses the assumption that $\mathcal{G}$ is a statistical sample path envelope for the process D^e. □

Remark: This is an amendment to Theorem 1 [39].

We can use Theorem 2 to compute the minimum battery size B^* satisfying a target loss of power probability ϵ^* by bounding $\Pr\{l(t) > 0\}$ with ϵ^*. We observe that the first term, $\Pr\{x^c(t) > 0\}$, in the minimum expression of Eq. (3.7) is independent of the battery size. We can therefore set battery size B^* to be zero whenever the first term forms the minima. Intuitively this means that there is no need of a battery if the probability of power outage is less than ϵ^*.

We use the envelope fitting approach described in Sec. 2.2 to compute the battery sizes using Theorem 2. If $\mathcal{G}$ is a statistical sample path envelope on the effective demand in the sense of Eq. (2.9) with bounding function ε_g, then using Eq. (3.7), we get

$$\min\left(Pr\{x^c(t) > 0\}, \varepsilon_g\left(B - \sup_{\tau \geq 0}(\mathcal{G}(\tau) - C\tau)\right)\right) = \epsilon^*$$

$$\implies B^* \leq \left(\sup_{\tau \geq 0}(\mathcal{G}(\tau) - C\tau) + \varepsilon_g^{-1}(\epsilon^*)\right) I_{(\Pr\{x^c(t)=1\}>\epsilon^*)} \qquad (3.11)$$

where I_{expr} is the indicator function, which is 1 if $expr$ is true and is 0, otherwise.

3.3.3 Battery Sizing in the presence of genset

Sometimes a genset is used in addition to a battery to guarantee that there will be no loss of power. For such a hybrid system, at any instant that the grid is unavailable, the demand can be either served by the remaining battery charge or by the genset. If the genset is large enough, there will be no loss of power as genset can be always used to meet the load. However, it is desirable to reduce carbon emission from a genset by using a battery to store 'greener' energy produced by the grid and using it when an outage occurs.

The allocation of demand between genset and the battery must first minimize the total loss of power, and then attempt to reduce the carbon emission from genset. Scheduling is trivial if the genset size is larger than the maximum (worst-case) demand load (i.e., $\max_t d(t)$). This is because we will have zero loss of power (as genset can always meet the load) and carbon emission is minimized by always scheduling energy from the battery whenever it is not empty. The scheduling, however, is non-trivial if the genset size is smaller than the maximum demand load. This is illustrated by the following example.

Suppose the aggregate load is fixed to 100kW for 5 successive hours when power from the grid is unavailable. Assume the battery is fully charged to its capacity of 100kWh at the beginning of the first hour and genset serves demand up to the rate of 80kW. If the battery is used merely to meet the load in the first hour, there will be a loss of power in the remaining 4 hours as genset cannot meet load > 80kW (see Figure 3.3a) and the battery is already exhausted. On the other hand, if genset is being used to its capacity for all the 5 hours with battery supporting the remaining 20kW every hour, there will be no loss of power (see Figure 3.3b)! Consequently,
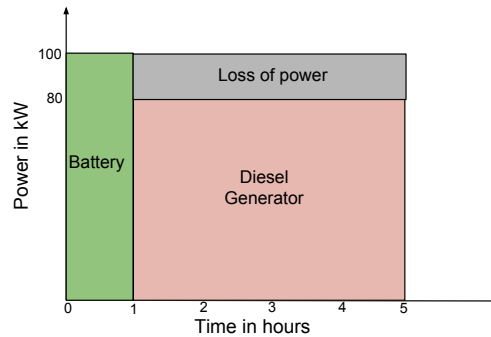
(a) Loss of power
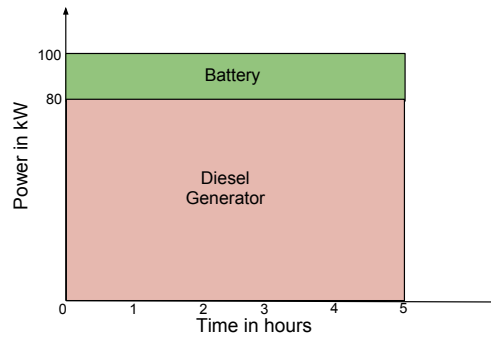
(b) No loss of power

Figure 3.3: An example showing non-triviality of power scheduling when genset maximum power rate is less than the maximum hourly demand. The battery size is 100kWh and genset capacity 80kW is less than the load 100kW.

as this example shows, if genset size is less than the maximum load $(\max_t d(t))$ exhausting the battery before using the genset is not the optimal strategy since that may lead to a larger loss of power.

For simplicity, therefore, we can assume that the genset capacity is large enough to meet the maximum aggregate load (Assumption 2). This is reasonable because the marginal cost of increasing genset capacity is small compared to the battery storages.

The objective in battery sizing in the presence of genset is to keep the carbon emission below a certain threshold. The carbon emission is proportional to the cumulative demand that cannot

be served by the battery when the grid is unavailable or

$$\text{carbon emission} \sim \sum_t l(t) \, . \tag{3.12}$$

Using the analogy between queueing theory and the distribution power system, this quantity corresponds to the total loss in a finite-buffer queue. In spite of extensive efforts, the problem is still open for non-Poisson arrivals. The complexity of the problem arises from the fact that the total loss is a function of the number and length of the busy periods, which occurs in a total time interval. Liu and Cruz [27] show that a probabilistic upper bound on the total loss must account for the numbers and lengths of the busy periods leads to cumbersome formulations, which cannot be used in practice.

Here we compute an upper bound on the expected value of the total loss (carbon emission) in a time interval of size T using Eq. (3.6) as follows:

$$\begin{aligned}
E\left[\sum_{t=1}^{T} l(t)\right] &= \sum_{t=1}^{T} E[l(t)] \\
&\leq \sum_{t=1}^{T} E\left[\min\left(d(t)x^c(t), \max_{0 \leq s < t}\left([D^e(s,t) - C(t-s) - B]_+\right)\right)\right] \tag{3.13} \\
&\leq \sum_{t=1}^{T} \min\Bigg(E\left[d(t)x^c(t)\right], \\
&\qquad E\left[d(t)x^c(t) I_{\max([D^e(s,t) - C(t-s) - B]_+ > 0]}\right]\Bigg) \tag{3.14} \\
&\leq \sum_{t=1}^{T} \min\left(E\left[d(t)x^c(t)\right], E\left[d(t) I_{\max([D^e(s,t) - C(t-s) - B]_+ > 0]}\right]\right) \tag{3.15} \\
&\approx \min\Bigg(\sum_{t=1}^{T} E\left[d(t)x^c(t)\right], \\
&\qquad T.E[d(t)].\Pr\{\max\left([D^e(s,t) - C(t-s) - B]_+\right) > 0\}\Bigg), \tag{3.16}
\end{aligned}$$

where we use Eq. (3.6) to obtain Eq. (3.13). The first term in Eq. (3.14) is trivial as it is the first term in the minima of the previous line. To obtain the second we use the definition of indicator function I, and the fact that $0 \leq x^c(t) \leq 1$. Finally, we assume that the two processes
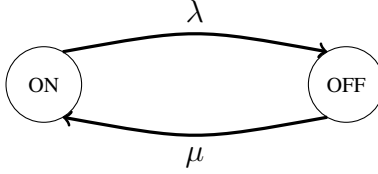
Figure 3.4: Modeling the grid availability process

in the second term in Eq. (3.15) are independent to derive Eq. (3.16). This assumption holds for statistically independent increments processes, which is widely assumed in the literature (e.g., Kelly [22]). In addition, we numerically find that the inaccuracy due to this approximation step is small.

We numerically find that the upper bound used to derive Eq. (3.14) from Eq. (3.13) is also quite tight. More precisely, we observe that Eq. (3.6) evaluates to its first term if the second term is positive.

Eq. (3.16) can be used for battery provisioning in the presence of genset and when the objective function is to minimize carbon emission.

3.4   Constructing an envelope for the effective demand

To evaluate our derivations, we use half hourly electricity consumption data from more than 4500 Irish homes produced as part of CER Smart Metering Project [9]. We assume that all the homes are from the same region. The effective demand from Eq. (3.2) is derived from randomly selected 100 homes in this dataset. Since we could not find an available trace for grid availability, we use a simple model to represent that process. We discuss that in the following section.

3.4.1   Modeling grid availability process

We model the grid availability process by an ON-OFF Markov model, where the grid is available in the 'ON' state and is unavailable in the 'OFF' state (see Figure 3.4). The transition rates between $ON \rightarrow OFF$ and $OFF \rightarrow ON$ are, respectively, λ and μ. With these parameters, on average, the grid spends $\frac{\lambda}{\lambda+\mu}$ and $\frac{\mu}{\lambda+\mu}$ fraction of time, respectively, in the OFF and ON states.

The stability condition in our problem enforces the long-term average rate of the demand during an average-length OFF state to be less than the average charging that the battery receives from the grid during an average-length ON state. That is, if L represents the long-term average rate of the demand (i.e., $L = \frac{\sum_{t=1}^{T} d(t)}{T}$), then

$$\frac{\lambda}{\lambda + \mu} L \leq \frac{\mu}{\lambda + \mu} C \implies \rho' L \leq C , \tag{3.17}$$

where $\rho' = \frac{\lambda}{\mu}$.

In our numerical studies we consider one of two cases: (1) We assume that we have a measurement trace of the effective demand (2) We assume that we have a multi-state Markov model for the demand.

Recall that the effective demand is the product of the demand (for which we have a measurement trace) added to the battery charging rate and the grid unavailability process. For the former case, where we need a measurement trace for the effective demand, we construct sample trajectories using the ON-OFF grid availability process. We construct a separate grid availability trajectory for each trajectory of the demand. To have a large enough dataset, we simulate 100 different sample paths of effective demand of a housing complex of 100 homes.

For the second case, where we assume a multi-state Markovian (MSM) process for the effective demand, we use the approach from [1]. As effective demand is zero whenever the grid is available ($x^c(t) = 0$), we first classify only the demands at all time slots with power outages into M Markovian states using the k-means clustering algorithm (we choose $M = 5$). Then, we add a new state representing availability of the grid. The emission rate of this state is 0 and we are at this state whenever the grid is available. We add C to the old values of the emission rates of the other states. The transition rate, q_{ij}, from state i to state j for such an $M + 1$ multi-state Markov chain can be calculated from the dataset using

$$q_{ij} = \frac{\text{Number of transitions from state } i \text{ to state } j}{\text{Total time spent in state } i}$$

3.4.2 Choosing parameters for $\mathcal{G}$ and ε_g

We use a leaky-bucket envelope $\mathcal{G}(t) = \sigma + \rho t$ with design parameters $\rho, \sigma \ (\geq 0)$ as a statistical sample path envelope for the effective demand in the sense of Eq. (2.9) with bounding function

ε_g. The design parameters in this modeling are the value of σ and ρ and the choice of distribution for ε_g. Empirically, we try different values of the leaky bucket parameters to find the minimum upper bound on the optimal battery size B^* using Eq. (3.11), i.e.

$$B^* \leq \min_{\rho \leq C; \sigma} \left(\sigma + \varepsilon_g^{-1} \left(\epsilon^* \right) \right) I_{(\Pr\{x^c(t)=1\}>\epsilon^*)} \tag{3.18}$$

For the bounding function ε_g, we recall that this is the CCDF on the event $\sup_{0 \leq s \leq t}([D^e(s,t) - \mathcal{G}(t-s)]_+)$. We observe that there is a large fraction of the elements evaluated as zero in that event. This happens with probability p_0 and consists of the cases where the arrival process D^e does not exceed the leaky bucket envelope. Let $\delta_0(x)$ be the delta function, which is 1 when $x = 0$, and is 0, otherwise. We can now write ε_g using the delta function as:

$$\varepsilon_g(x) = p_0 \delta_0(x) + (1 - p_0)\varepsilon_\delta(x)$$

or

$$\forall x > 0 : \quad \varepsilon_g(x) = (1 - p_0)\varepsilon_\delta(x) \tag{3.19}$$

where ε_δ is a CCDF function with $\varepsilon_\delta(0) = 1$ [4]. Eq. (3.18) can now be rewritten as:

$$B^* \leq \min_{\rho \leq C; \sigma} \left(\sigma + \varepsilon_\delta^{-1} \left(\frac{\epsilon^*}{1 - p_0} \right) \right) I_{(\Pr\{x^c(t)=1\}>\epsilon^*)} \tag{3.20}$$

We first tried fitting an exponential distribution to the function ε_δ, but the distribution failed to pass the Kolmogorov-Smirnov (KS) fitting test (we always use the default MATLAB parameters, i.e. hypothesis rejected at 0.05 significance level). The quantile-quantile (Q-Q) plots show heavy under-estimation around the tail (see Figure 3.5). Therefore, we use either of the following more complicated distributions:

1. **Weilbull distribution:** For parameters a and b (> 0), Weibull distribution is given as

$$\varepsilon_\delta(x) = abx^{b-1}e^{-ax^b}$$

   We use the default MATLAB function *wblfit* to find the parameters a, b, and find that the distribution passes the KS fitting test (see Figure 3.5).

---

[4]For convenience, we overload the term bounding function to also refer to ε_δ
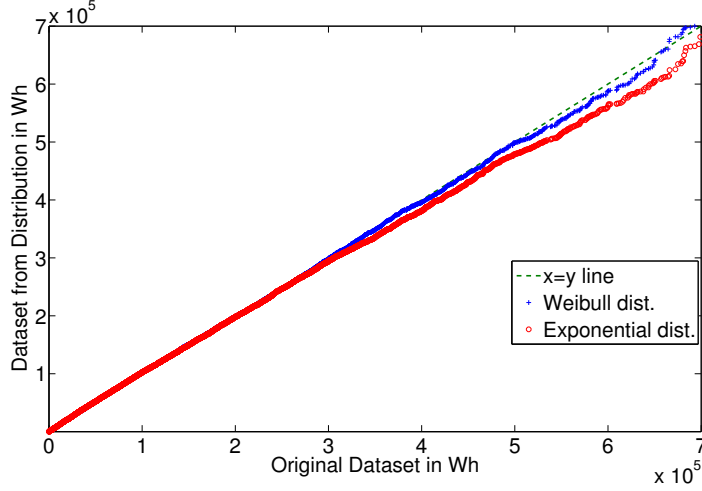
Figure 3.5: Q-Q plots for evaluating exponential and Weibull distribution as tail bound candidates

2. **Hyper-exponential distribution:** Although Weibull distribution is a good fit for the tail bound distribution, because of its heavy-tailed property, it is less preferable than hyper-exponential distribution. We therefore try fitting a two-phase hyper-exponential distribution with three parameters, p, β_1, β_2, i.e.

$$\varepsilon_\delta(x) = pe^{-\beta_1 x} + (1-p)e^{-\beta_2 x}$$

To fit hyper-exponential distribution to dataset X, we use the standard approach [26] of empirically trying different values of parameter p and finding the corresponding values of parameters β_1 and β_2 by matching the first and the second order moments, i.e.

$$E[X] = \frac{p}{\beta_1} + \frac{1-p}{\beta_2} \tag{3.21}$$

$$E[X^2] = \frac{2p}{\beta_1^2} + \frac{2(1-p)}{\beta_2^2} \tag{3.22}$$

We perform KS fitting test to check the validity of the obtained parameters.

The approach used to model D^e in this section can also be employed to model the demand thus facilitating a generic performance analysis for intermittent demand energies.

24

3.5   Numerical results

In the following section we compare our battery sizing approach with the optimal benchmark for the same dataset as in Section 3.4. We use the Markov-modulated ON-OFF process as described in Section 3.4.1 to generate grid unavailability trace. Unless otherwise stated, we use the parameters $\mu = 1\ hr^{-1}$ and $\lambda = \frac{1}{11}\ hr^{-1}$, which correspond to an average of two power outages in a day with average duration of a power outage being one hour, which is common for developing countries such as India. Moreover, unless otherwise stated, the target violation probability in examples is assumed to be one day loss of power in ten years, i.e. $\epsilon^* = 2.7 * 10^{-4}$ and battery charging rate $C = 100$ kW.

3.5.1   Battery sizing in the absence of genset

In this section we tend to evaluate our upper bound formulation on the battery sizing in the absence of genset from Section 3.3.2 and our effective demand modeling from Section 3.4. The evaluation is carried out by comparing the battery sizing from our modeling and formulations with the benchmark and existing methods as described below

- *Dataset quantile*: This is the battery sizing obtained by using the effective demand measurement trace as the input to the exact recursive loss of power description in Eq. (2.3). The battery size obtained by this method is the least value that satisfies the target loss of power probability given the knowledge of entire demand trace.

- *Our bound*: Here, we use the parameter fitting techniques as explained in Section 3.4.2. We use leaky-bucket as the statistical sample path envelope on D^e and fit a hyper-exponential (or Weibull) distribution on ε_δ. Using Theorem 2 for loss of power formulation, we find the least battery size that satisfies the target loss of power probability (as given in Eq. (3.11)).

- *Ideal D^e model*: Here, we apply the effective demand measurement trace to Eq. (3.9) for loss of power formulation and find the least battery size that satisfies the target loss of power probability. By avoiding to use Theorem 2 in this approach, we remove the inaccuracy imposed by D^e modeling (i.e. from Eq. (3.9) to Eq. (3.10)). This allows to distinguish between the inaccuracy that is induced by D^e modeling and that from Theorem 2.
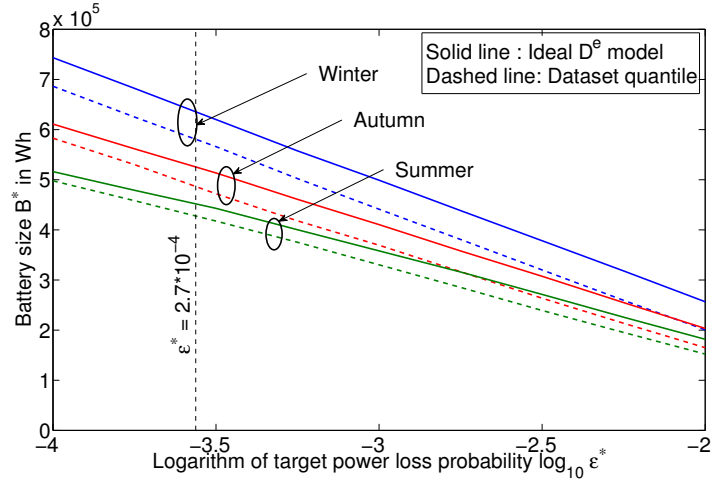
Figure 3.6: **Accuracy of loss of power formulation:** *Dataset quantile* and *Ideal D^e model* battery sizes as a function of target violation probability in three seasons for Irish demand dataset with ON-OFF grid unavailability with parameters $\mu = 1\ hr^{-1}$ and $\lambda = \frac{1}{11}\ hr^{-1}$

- *Kesidis bound*: Here, we first compute a deterministic peak-rate constrained leaky-bucket description for the effective demand process in the sense of Eq. (2.7). We then use the Kesidis battery overflow probability from Eq. (2.8) for loss of power formulation and find the least battery size that satisfies the target loss of power probability.

- *MSM bound*: We obtain the statistical sample path envelope for the arrival process D^e by first modeling it as a multi-state Markovian process as discussed in Section 3.4.1. Then we insert the statistical sample path envelope for Markovian processes from Section 2.2 in the loss of power formulation in Theorem 2 to obtain bounds on the battery size.

To study the accuracy of our analysis and possible sources of inaccuracy we must consider two major issues (1) how accurately we could model the effective demand using envelopes, (2) how accurately our formulation can compute the loss of power or carbon emission values given that there is no inaccuracy in modeling the effective demand. We study each issue in turn next.

Accuracy of our loss of power formulation

The accuracy of our loss of power formulation can be examined by the comparison of 'dataset quantile' that uses the dataset trace and exact recursive loss equation with 'Ideal D^e model', which also uses the dataset trace but applies the dataset to our upper bound loss formulation in Eq. (3.9). Figure 3.6 illustrates this comparison as a function of the target violation probability ϵ^*. To model accurately the fluctuations of the demand we consider battery sizing for different weather seasons by dividing the demand dataset into three seasons: Winter (December-March), Summer (April-July), and Autumn (August-November). We compute the battery size for each season separately. Note that a battery size that satisfies the loss of power requirements throughout the year would be the maximum of the battery sizes among all seasons.

We first observe from Figure 3.6 that for one day in ten years target loss of power probability (i.e., $2.7 * 10^{-4}$), 'Ideal D^e model' is within 10% of 'dataset quantile' implying that our loss of power formulation is reasonably tight. We also notice that different seasons can have significantly different battery size requirements probably due to power-hungry heating appliances used in cold weather. A significant difference (around 35%) in the battery sizes can be seen between Summer and Winter seasons.

Our loss of power formulation in Eq. (3.7) consists of the minimum of two terms. The first term $\Pr\{x^c(t)\} > 0$ states that the loss of power formulation at any time instant cannot be larger than the power outage probability. This is a trivial bound, which becomes the dominant term in the minimization when the battery size is not large (to see the effect of this term one can consider the extreme case of battery-less scenario). The second term in Eq. (3.7) is quite accurate in identifying loss of power events, i.e. $\Pr\{l(t) > 0\}$ as can be seen in Figure 3.6 .

Finally, we note that while hyper-exponential distribution is sufficient to characterize seasonal demand as it passes KS-test, it seems to be an invalid distribution to describe the annual demand. This is due to seasonal changes of home-load, such as average demand, especially due to heating and cooling elements, which exhibit non-exponential, possibly heavy-tailed, behaviour.

Accuracy of D^e modeling

We evaluate the performance of the fitting technique in modeling D^e by comparing the battery sizes obtained by this model and those from 'dataset quantile' and 'Ideal D^e model'. In fact, the difference between the battery sizing by envelope fitting with that of 'Ideal D^e model' indicates
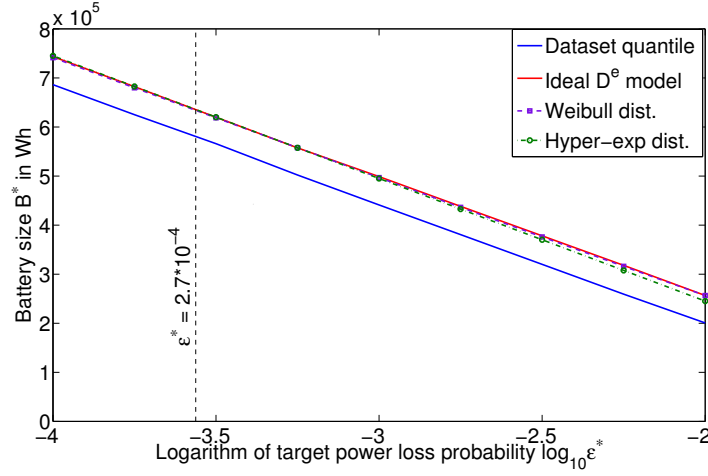
27

Figure 3.7: **Accuracy of D^e modeling:** Minimum battery size B^* as a function of violation probability ϵ^* for Irish demand dataset and with ON-OFF grid unavailability with parameters $\mu = 1 \ hr^{-1}$ and $\lambda = \frac{1}{11} \ hr^{-1}$

the accuracy of fitting since the 'Ideal D^e model' shows the battery sizing scheme when the D^e modeling inaccuracy is eliminated. We study both Weibull and hyper-exponential as tail bounds in the examples in this section. We study the effect of different key parameters on the accuracy of fitting by conducting a thorough sensitivity analysis of the above methods.

Figure 3.7 compares the battery size computed using the methods as a function of the violation probability. The similar slopes observed from this figure for different methods implies that the ratio of the battery sizes from each pair of methods is almost fixed even as the violation probability is varying.

Figure 3.8 illustrates the battery sizing as a function of battery charging rate C with a target violation probability $\epsilon^* = 2.7 * 10^{-4}$. As the battery charging rate increases, all curves converge to the battery size required by an ideal battery, which can be charged instantaneously. The battery required for this ideal case must be large enough to serve the demand during the time when the grid is unavailable.

Finally, Figure 3.9 shows the battery sizing from different methods as a function of the ratio of grid ON-OFF parameters. We set average power outage duration to be one hour, i.e. $\mu = 1 \ hr^{-1}$, and only vary λ. Due to limited space, we don't show error bars for 'Ideal D^e model' and 'Weibull distribution'. We observe that even for very high power outage periods, like $\rho' = 0.33$

28

Figure 3.8: **Accuracy of D^e modeling:** Minimum battery size B^* as a function of battery charging rate C for a fixed target loss of power probability $\epsilon^* = 2.7 * 10^{-4}$ for Irish demand dataset and with ON-OFF grid unavailability with parameters $\mu = 1 \ hr^{-1}$ and $\lambda = \frac{1}{11} \ hr^{-1}$

(25% power outage), the bounds are within 15% of the 'Dataset quantile'.

This sensitivity analysis indicates that our D^e modeling and loss of power formulations are quite tight.

Comparison to Kesidis and MSM

In this section, we evaluate the loss of power formulation from Theorem 2 with those obtained from other existing techniques: 'Kesidis bound', and multi-state Markov chain 'MSM'. We have also included 'Dataset quantile', and 'our bound using hyper-exponential distribution' as benchmarks. Figure 3.10 compares the battery sizes computed by the above methods as a function of the violation probability. We find that our approach out performs the competing approaches. It can also be observed that the Kesidis bounds are almost insensitive to the violation probability for the range of study. This is due to loss of power formulation in Eq. (2.8), which suggests the battery size as a function of ϵ^* to be:

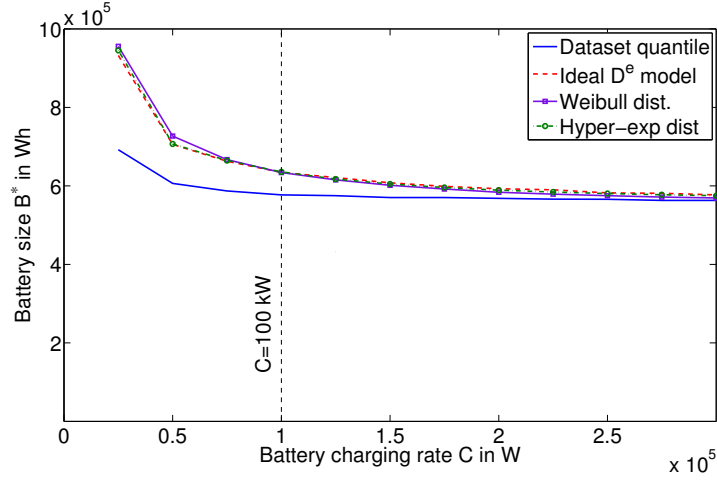$$ B = \frac{\sigma\left(1 - \epsilon^* \frac{C}{\rho}\right)}{\frac{\pi - \rho}{\pi - C} - \epsilon^*} \ . $$

29
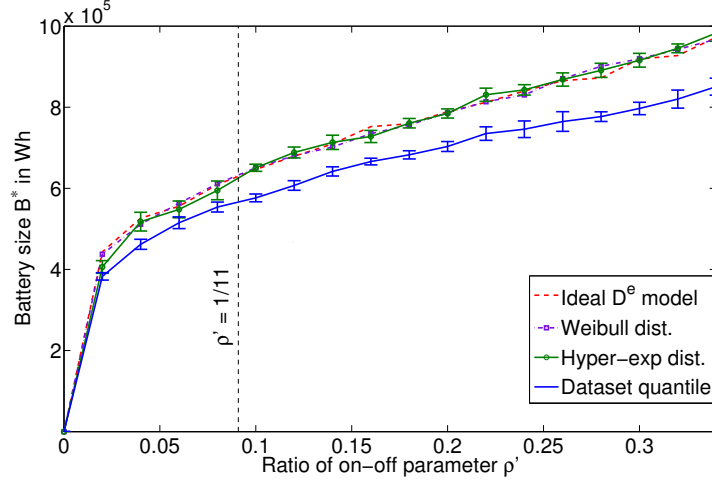
Figure 3.9: **Accuracy of D^e modeling:** Minimum battery size B^* as a function of ρ' for a fixed target loss of power probability $\epsilon^* = 2.7 * 10^{-4}$ for Irish demand dataset and with ON-OFF grid unavailability with parameter $\mu = 1 \; hr^{-1}$

The impact of varying ϵ^* on the resulting B from the above equation is only noticeable when ϵ^* is comparable to $\frac{\rho}{C}$ or $\frac{\pi-C}{\pi-\rho}$, which is not the case for the range of values in Figure 3.10. The Kesidis bound is comparably loose since it is based on the assumption that the effective demand is regulated, which requires a deterministic peak-rate constrained leaky-bucket envelope on the effective demand. The tightness of Kesidis bound is highly affected by how tight the deterministic envelope is in describing the regulated traffic. The more bursty the traffic is, the looser the bound would be. Moreover, the MSM bound is also not as tight as the envelope fitting and this is due to the inaccuracy induced by employing the union bound to compute a statistical sample path envelope (Eq. (2.15)) for the exponentially bounded burstiness processes (including MSM processes) as also observed in [7].

3.5.2 Battery sizing in the presence of genset

For battery sizing in the presence of a genset, we study the accuracy of our carbon emission bounds as a function of the battery size. We use Eq. (3.12) as the metric of carbon emission. The plots of this section show the following curves:

30

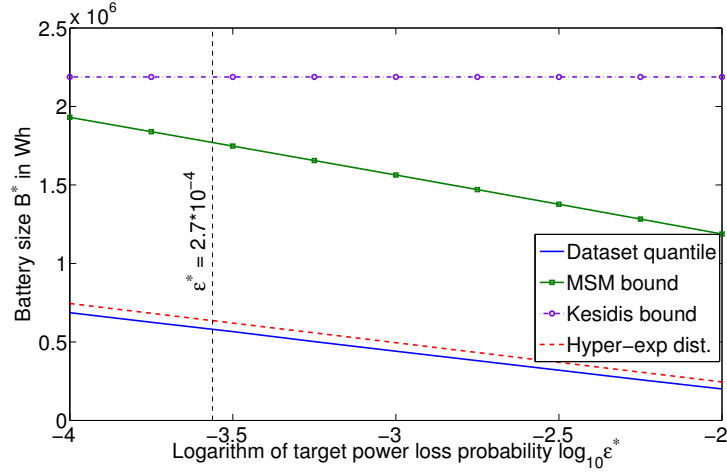Figure 3.10: **Comparison with other bounds:** Minimum battery size B^* as a function of battery charging rate C for Irish demand dataset and with ON-OFF grid unavailability with parameters $\mu = 1\ hr^{-1}$ and $\lambda = \frac{1}{11}\ hr^{-1}$

- *Dataset quantile*: Similar to the 'Dataset quantile' in the absence of genset, we apply the dataset trace to Eq. (3.12) and compute the exact carbon emission for our dataset.

- *Our bound*: This is the upper bound on carbon emission from Eq. (3.16) and using envelope fitting as explained in Section 3.4.2 to model D^e with hyper-exponential distribution on ε_δ.

- *Ideal D^e model*: We remove the inaccuracy induced by D^e modeling by applying the dataset trace directly to Eq. (3.15) to compute upper bounds on carbon emission.

We compute the carbon emission as a function of the battery size for charging rate of $C = 100$ kW in Figure 3.11. For any given carbon emission threshold, one can use this plot to compute the required battery size. The plot is divided into three regions I, II, and III. Region I corresponds to the case where Eq. (3.16) is evaluated to $\sum_{t=1}^{T} E[d(t)x^c(t)]$, which is the battery-less scenario. If the carbon emission target threshold is as large as any value in this region we can remove the battery. Region II corresponds to the case when $C > B$. If the target carbon emission threshold falls into this region, one might choose the battery size to be equal to the energy generated in one time slot with the charging rate, i.e., $B = C$. Finally, Region III corresponds to the case of $C < B$ for which the curves in that region must be used to size the battery.

31

Figure 3.11: **Battery sizing in the presence of genset:** Carbon emission from genset as a function of battery size B for Irish demand dataset and with ON-OFF grid unavailability with parameters $\mu = 1 \ hr^{-1}$ and $\lambda = \frac{1}{11} \ hr^{-1}$

From Figure 3.12 we can see that our bound becomes more accurate for larger charging rates. Even for a relatively small charging rate like 100 kW, we find that our bound is within a factor of 1.7 from the 'dataset quantile'. We can observe from Figures 3.11-3.12 that the carbon emission using Eq. (3.16) are slightly below the 'Ideal D^e model'. This is because of the independence assumption made for 'our bound' in Eq. (3.16) and 'Ideal D^e model' does not have that assumption.

3.6 Conclusions

Motivated by the need to mitigate against the loss of grid power, we present an analytical technique based on the stochastic network calculus to compute the battery size needed for a housing complex connected to an unreliable grid to ensure a given target loss of power probability. Numerical evaluations show that the sizing using our methodology is within 10% of the minimum battery size required had the future load been exactly known. In contrast, the battery size computed using classical methods is far larger than necessary.

Recognizing that the conventional approach to generate backup power is using diesel gener-
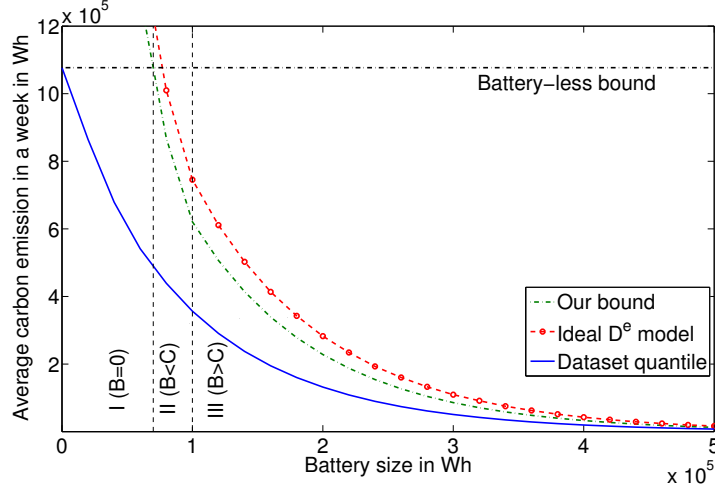
32
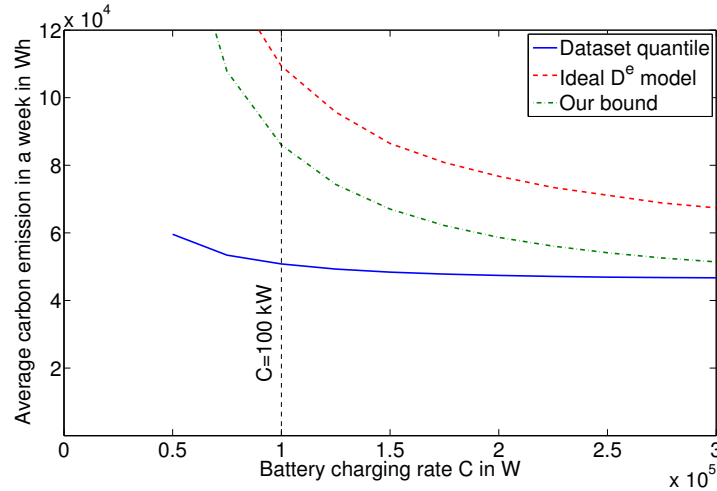
Figure 3.12: **Battery sizing in the presence of genset:** Carbon emission from genset as a function of battery charging rate C for Irish demand dataset with ON-OFF grid unavailability with parameters $\mu = 1 \ hr^{-1}$ and $\lambda = \frac{1}{11} \ hr^{-1}$, and constant battery size $B = 3 * 10^5 Wh$

ators, we also study the trade-off between the size of a battery and the carbon emission due to genset operation. For a given battery size, our computation of the carbon emission is within a small factor (1.7) of the value obtained through numerical evaluation. This allows us to find the minimum battery size needed to bound the carbon footprint of a diesel generator. This is not only a useful result in its own right, but given that prior work in the area of teletraffic analysis has had limited success in computing upper bound on the total loss of buffer for non-Poisson arrivals, we believe that our work is of general interest even in the area of teletraffic analysis.

Our results are necessarily limited by the lack of demand and outage data from developing coun- tries. We model the demand from a neighbourhood of homes in a developed country by the demand of 100 randomly selected Irish homes and we assume that outages are modeled by a two-state Markov model. These limit the strength of our numerical results. Nevertheless, our general approach can be used to study real datasets when they are available.

Chapter 4

Using battery to decrease genset fuel consumption

There are many remote villages in developing countries, such as India, that are not electrified and where extending the grid is difficult [33]. The problem of a lack of power grid is also common for mobile base stations located in remote areas [36]. Even when there is a grid connectivity, the grid is prone to failures due to various reasons such as storms and equipment failures. In developing countries, load shedding lasting two-to-four hours is common because of a large gap between energy supply and demand [31]. Thus a small community or industry may decide to go off-grid for higher power reliability. These places that are off-grid often install a diesel genset to meet their demands. In this work, we study how to use a hybrid genset-battery system to improve the fuel consumption efficiency of the genset.

4.1   Motivation and Related Work

The efficiency of a genset is known to be the greatest when it operates close to its capacity (also called rated or nominal power) G. In complete absence of a grid, a genset is usually sized to meet the occasional peaks of a stochastic demand. This causes the genset to mostly operate at low efficiency to meet demands only around $30\% - 60\%$ of its rated capacity. Continued operation of genset to meet small demands can also lead to engine damage [19]. However, a battery can be used to increase the average fuel consumption efficiency of the genset. As

explained in Section 4.2.1, the hybrid system operates in one of the following three modes: (a) demand met by battery only, (b) demand met by genset only, and (c) demand simultaneously met by battery and genset [16].
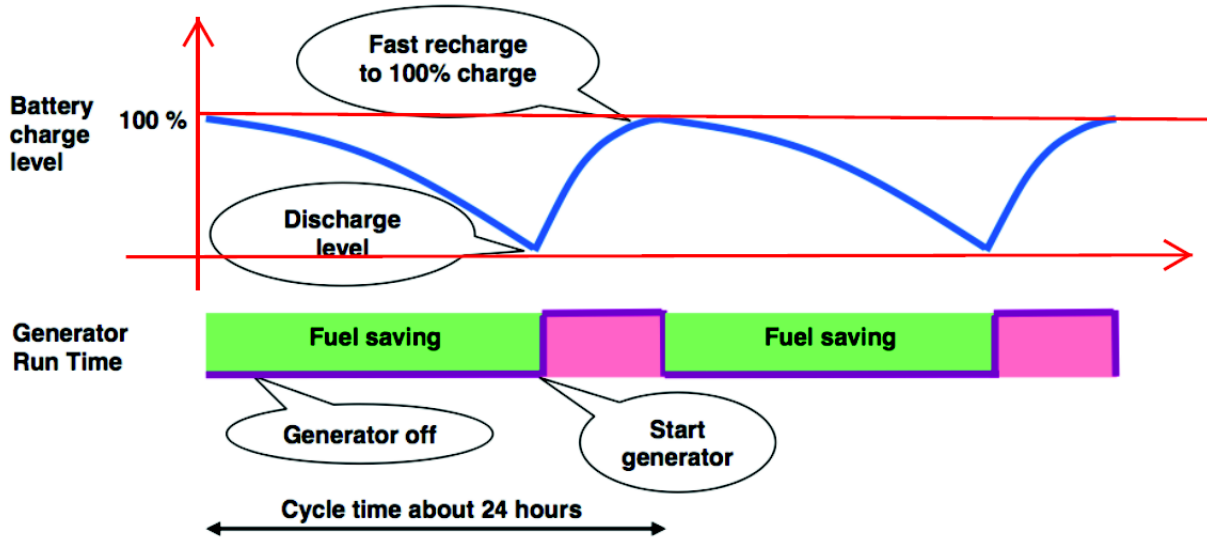
Figure 4.1: Use of battery to decrease genset fuel consumption [36]

An accurate expression describing the rate of genset fuel consumption for a demand $d(t)$ is given by the following affine function

$$k_1 G + k_2 d(t) \tag{4.1}$$

where k_1 and k_2 are some constants [37][4]. This motivates us to improve efficiency of the genset using a battery in the following two ways. Firstly, mode (c) tells that we can simultaneously run genset and discharge battery to meet loads. As a typical battery's discharge rate is high, this avoids over-sizing the genset to meet occasional peak loads, and hence increases genset efficiency. Secondly, at times of low demand, the genset can be turned off by meeting the demand entirely from the battery. When the demand is high (but less than the genset capacity G), a running genset is used to meet both the demand and recharge the battery. This increases efficiency as the genset operates closer to its capacity (see Figure 4.1).

These methods of using a battery to improve genset efficiency motivates us to study the following two problems:

(i) **Battery-usage problem:** For a small industry (community) that is off-grid and uses a genset to meet its demand, we study how to size the battery and schedule power from the battery-genset hybrid system to minimize the total fuel consumption .

(ii) **Going off-grid problem:** For an industry (community) that is currently on-grid but decides to go off-grid, we address the problem of using a battery to prevent over-sizing of the genset. We use tools from stochastic network calculus to size the battery and the genset such that the loss of load probability due to the demand exceeding the genset capacity and the battery being empty is less than a threshold ε^* .

4.2   System Model

We assume a discrete time model, where time-slot t represents the time interval $[t-1, t)$. Practically, the length of the time slot should neither be very small, as it increases the size of the numerical computation, and nor very large because then the discrete system is not an accurate description of the continuous system. We are also constrained by the time taken to turn a genset on after it has been turned off. For applications in smart grid, we suggest a time slot duration around $5-15$ mins.

Name	Description
G	Maximum genset power production rate
B	Battery storage capacity
C	Maximum battery charging rate
$d(t)$	Demand in time slot t
$b(t)$	Battery level of charge at time t
ϵ^*	Target loss of power probability
$x(t)$	Indicator variable for genset at time t

Table 4.1: Notation

Let $x(t)$ be an indicator variable, which is 1 if the genset is operating in time-slot t and is 0 otherwise. Let $d(t)$ represent the demand in time-slot t, and let $b(t)$ represent the battery level

at the end of time-slot t. We assume a simple battery model where the charging rate is at most a constant C ($\leq G$) and is independent of the battery size B and also of its state of charge. To ensure that there is no external source of energy, we always assume that the battery state of charge at the beginning of slot 1 and at the end of slot T is zero, i.e. $b(0) = b(T) = 0$.

4.2.1 Three modes of hybrid system operation

The genset-battery hybrid system that we consider can operate in three modes to meet the demand with the following changes to the battery state of charge (see Figure 4.2).

a) **Demand met by battery only:** The battery is discharged to meet the demand while the genset remains turned off.
$$b(t) = [b(t-1) - d(t)]_+$$

b) **Demand met by genset only:** The genset is turned on and it simultaneously meets the demand and charges the battery. Any demand greater than the capacity of genset G cannot be met in this state.
$$b(t) = \min\{B, [b(t-1) + \min\{G - d(t), C\}]_+\}$$

c) **Demand simultaneously met by battery and genset:** The genset is turned on and the battery is discharged simultaneously to meet the demand.
$$b(t) = [b(t-1) - (d(t) - G)]_+$$

4.2.2 Definitions

- **Demand profile $\mathcal{D}$:**
  We define demand profile $\mathcal{D} = \{d(1), d(2), \ldots, d(T)\}$ to be the set of demands for T consecutive time slots.

- **Genset scheduling strategy:**
  Given demand profile $\mathcal{D}$, battery size B, and charging rate C, a genset scheduling strategy is an algorithm that computes a unique set $\mathcal{S} \subseteq \{1, 2 \ldots, T\}$, called genset scheduling, which denotes the set of time slots when the genset is turned on to meet the demand

37

and/ or charge the battery. We sometimes also refer to the strategy by set $\mathcal{S}$ to simplify notation. The strategy is called online (offline) if the decision about time t is independent (dependent) of demands after time t.

- **Feasible scheduling $\mathcal{S}$:**
  For any demand profile $\mathcal{D}$, battery size B, and charging rate C, we define a genset scheduling strategy $\mathcal{S}$ to be feasible if the following holds:

  1. The genset-hybrid system is always in one of the three modes defined in Section 4.2.1 and follows the battery state of charge equations.

  2. Loss of load is at most ε^* fraction of the time and the battery state of charge at the beginning of time slot 1 and at the end of time slot T is zero.

- *Genset-only* **scheduling**:
  A scheduling strategy where the genset is always on, i.e. $\mathcal{S} = \{1, 2, \ldots, T\}$.

- *Alternate* **scheduling**:
  A scheduling where the system alternates between running the genset until the battery is completely charged to its capacity B and using only the battery to meet the demand until it empties.

- **Competitive ratio α:**
  Given a battery size B and a charging rate C, for any genset scheduling strategy $\mathcal{S}$ we define the competitive ratio α (≥ 1) as

$$\sup_{\mathcal{D}} \frac{\text{Fuel consumption by feasible scheduling } \mathcal{S}}{\text{Fuel consumption by feasible offline optimal scheduling}}$$

4.3 Battery-usage

As discussed in Section 4.1, the motivation behind this problem is to find a strategy for an industry, that already has a genset, to use a battery to reduce its fuel consumption. We therefore make the assumption that the size of the genset, G, is given and it is large enough to meet the peak demands. We also assume that the genset can simultaneously charge the battery at its peak charging rate C. For this problem we will have no loss of load, i.e. $\varepsilon^* = 0$, as the genset can
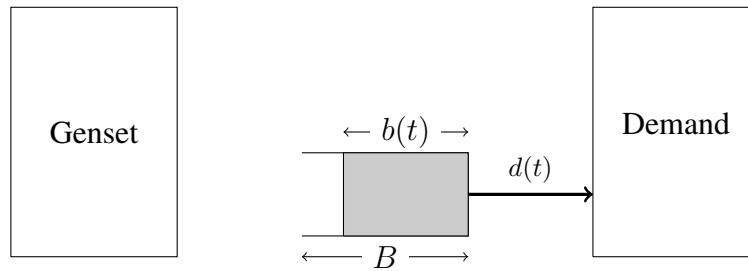
(a) Load met by battery only
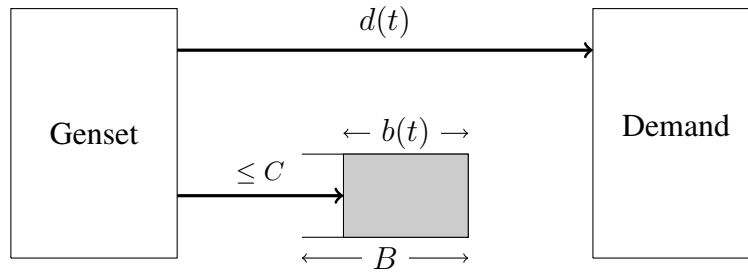
(b) Load met by genset only
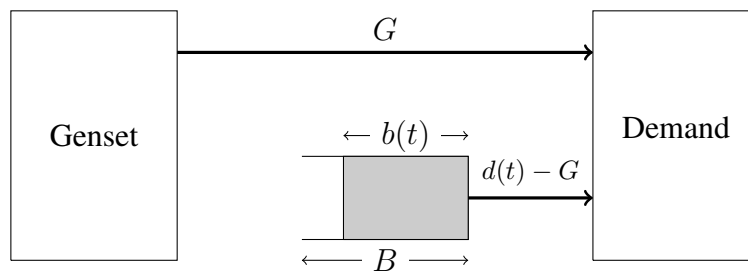
(c) Load simultaneously met by battery and genset

Figure 4.2: Model for the genset-battery hybrid system

be always turned ON to meet the demand. The goal is to size the battery and schedule power between the genset and the battery (battery-genset power scheduling problem) to minimize total fuel consumption.

4.3.1 Characterizing the offline optimal scheduling

For genset fuel consumption given by Eq. 4.1, we have the following theorem on battery-genset power scheduling.

Theorem 3. *Consider T consecutive time slots such that $b(0) = b(T)$. For a given genset and battery size, the problem of minimizing genset fuel consumption is equivalent to the problem of minimizing the number of time slots for which the genset is turned on.*

Proof. Let the genset be on in m out of T time slots and let $g(1), g(2), g(3), \ldots, g(m)$ denote the energy produced by the genset in those time slots. Since the state of energy in the battery at the beginning and the end is the same, conservation of energy gives $\sum_{1 \leq i \leq T} d(i) = \sum g(j)_{1 \leq j \leq m}$. Total fuel consumption by the genset is therefore given as

$$\sum_{1 \leq j \leq m} (k_1 G + k_2 g(j)) = m k_1 G + k_2 \sum_{1 \leq i \leq T} d(i).$$

Since for a given problem instance $k_1 G$ and $\sum_{1 \leq i \leq n} d(i)$ are already known, the problem of minimizing genset fuel consumption is equivalent to minimizing m, i.e. the number of slots for which the genset is on. $\qquad \square$

Using Theorem 3, the objective of the scheduling problem can be changed from minimizing total fuel consumption to minimizing the number of genset operation time slots. The offline optimal battery-genset power scheduling when loss of load probability $\varepsilon^* = 0$ is therefore given by the following mixed-integer program.

Objective:

$$\min_x \sum_{t=1}^{T} x(t) \tag{4.2}$$

Subject To:

$$b(t) \leq b(t-1) - d(t) + Gx(t) \tag{4.3}$$
$$b(t) \leq b(t-1) + C \tag{4.4}$$
$$0 \leq b(t) \leq B \tag{4.5}$$
$$x(t) \in \{0,1\} \tag{4.6}$$

When the battery is being charged, i.e. $x(t) = 1$, Constraint 4.3 ensures that the battery is charged by at most $G - d(t)$. Otherwise, i.e. $x(t) = 0$, it ensures that the battery is discharged by at least $d(t) - G$. Constraint 4.4 ensures that the battery charging rate is at most C. Constraints 4.5 are the capacity constraints on the battery. Constraint 4.6 imposes integrality on variables $x(t)$.

Although practical loads, battery sizes, and charging rates have values in a small range, for the sake of completeness we prove that the general battery-genset power scheduling problem is NP-hard. We reduce a general instance of $0 - 1$ Knapsack problem, a NP-hard problem, into our problem instance.

Knapsack problem: Given n objects of weights $w_1, w_2, \ldots, w_n$, a bag that can carry at most weight W, and a target value $P \leq n$, does there exist a subset of objects S such that $P \leq |S|$ and $\sum_{i \in S} w_i \leq W$.

Battery-genset scheduling problem: Given a battery of size $B \geq 0$, a battery charging rate $C \geq 0$, initial battery charge $B_0 \geq 0$, and demands $d(1), d(2), \ldots, d(T)$. Given a target value P, does there exist a genset schedule that turns on genset for at most $T - P$ time slots while ensuring that there is no loss of load.

Theorem 4. *Battery-genset scheduling problem is NP- hard.*

Proof. Let the battery size be $B = W$ and assume that it is fully charged at the beginning, i.e. $B_0 = W$. Let the battery charging rate be $C = 0$ and let the demands $d(t)$ for $1 \leq t \leq n$ be

41

$d(t) = w_t$. For the same target value P, the genset scheduling problem returns yes iff the original Knapsack problem returns yes. Thus, we have reduced the Knapsack problem to a Battery-genset scheduling problem, showing that the later problem is at least as hard as the former problem. $\quad\square$

4.3.2   Online Alternate scheduling

In Section 4.3.1 we assumed that future load is exactly known. In practice, however, prediction of stochastic demand is very difficult. Here we study alternate scheduling, an online scheduling strategy, where no assumption is made on the future demand. Later, in Section 4.5, we numerically show that for practical industrial loads alternate scheduling is close to the offline optimal.

Theorem 5. *If battery charging rate is sufficient to charge the battery in a single time slot, i.e.* $C \geq B$, *alternate-scheduling is optimal.*

Proof. We prove by contradiction and suppose that there exists an optimal offline scheduling different from alternate scheduling. We note that $C \to \infty$ implies that there exists an optimal offline scheduling that charges the battery fully to its capacity B in any time slot when the genset is on. Consider the first time slot t where the battery has sufficient charge to meet demand $d(t)$ but the optimal scheduling turns on the genset to meet the demand and charge the battery to B. Also, consider the earliest time slot $s > t$ when alternate scheduling turns on the genset because the battery is not sufficiently charged. Such a slot s exists as otherwise alternate scheduling will perform better than the optimal. After activation of genset in this slot s, the battery will be fully charged. Hence, at the end of slot s, alternate scheduling can be in a better state than the optimal to meet the future demand as the optimal will have a battery state of charge less than B. Also, both optimal and alternate have turned the genset on for the same number of time slots. This proves that alternate is an optimal scheduling. $\quad\square$

We next show that for our problem, where the genset size is large, the competitive ratio of alternate scheduling can be exactly computed. For better exposition, we avoid ceiling and floor functions by assuming G and B are divisble by C. This assumption can be easily removed.

Theorem 6. *If the genset is large enough to simultaneously meet the peak demand and charge the battery at its maximum rate C, competitive ratio for alternate scheduling is* $\frac{k_1 \frac{G}{C} + k_2}{k_1 + k_2}$.

Proof. Consider the worst case demand profile $\mathcal{D} = \{d(1), d(2), \ldots, d(n)\}$ such that the battery is empty at the beginning of slot 1 and at the end of slot n for alternate scheduling. Our modeling assumptions give $C \le G \le B$ and $d(i) \le G - C$ for all $i \in \{1, 2, \ldots, n\}$. Let m denote the number of cycles that the battery goes through in the n time slots.

Correctness: For alternate scheduling, the battery is always charged by the genset at its peak rate C. Hence the total number of charging time slots are exactly $m\frac{B}{C}$. Note that the alternate scheduling discharges the battery to meet mB demand. This means $\sum_{i=1}^{n} d(i)$ is at least mB. As there is no source of energy other than the genset, the optimal scheduling will turn the genset on for at least $\frac{\sum_{i=1}^{n} d(i)}{G} \ge \frac{mB}{G}$ time slots. Thus, using the definition of competitive ratio α (see Eq. 4.2), we get

$$\alpha \le \frac{k_1 G \frac{mB}{C} + k_2 \sum_{i=1}^{n} d(i)}{k_1 G \frac{mB}{G} + k_2 \sum_{i=1}^{n} d(i)}$$

Observe that this ratio is maximum when the same additive term in the numerator and the denominator, $k_2 \sum_{i=1}^{n} d(i)$, achieves its minimum value (since $\alpha \ge 1$). Using $\sum_{i=1}^{n} d(i) \ge mB$ again, we get

$$\alpha \le \frac{k_1 G \frac{mB}{C} + k_2 mB}{k_1 G \frac{mB}{G} + k_2 mB} = \frac{k_1 \frac{G}{C} + k_2}{k_1 + k_2}$$

Tightness: The worst case is achieved for a periodic demand profile, where the demand alternates between tending to zero for the first $\frac{B}{C}$ time slots and being $G - C$ for the next $\frac{B}{G-C}$ time slots. Let m be the number of periods in n time slots. In any period of the demand, alternate scheduling will turn on the genset for the first $\frac{B}{C}$ time slots and discharge the battery for the remaining $\frac{B}{G-C}$ time slots. The optimal scheduling will, however, always discharge the battery when the demand tends to zero. In each period of the demand being $G - C$ for $\frac{B}{G-C}$ time slots, the optimal turns the genset on to meet the demand and charge the battery for the first $\frac{B}{G}$ time slots, followed by discharging the battery to meet the demand for the remaining $\frac{BC}{G(G-C)}$ time slots. The ratio between fuel consumption by alternate and optimal is now given by

$$\frac{k_1 G m \frac{B}{C} + k_2 mB}{k_1 G m \frac{B}{G} + k_2 mB} = \frac{k_1 \frac{G}{C} + k_2}{k_1 + k_2}$$

$\square$

4.3.3 Savings

There are two conflicting objectives of installing a battery– minimizing carbon foot print (total fuel consumption) and minimizing the cost of the system. We compare both these objectives before and after the installation of a battery of size B. In absence of battery, the cost of the system is given exactly by the cost of fuel consumption (since the genset cost is a sunk cost, we ignore it). Here, total fuel consumption in time $[0, T]$ is the same as genset-only scheduling, i.e.

$$k_1 GT + k_2 \sum_{t=1}^{T} d(t)$$

We now estimate the number of time slots for which the genset is on after installation of a battery of size B and charging rate C due to alternate scheduling. As the genset is large enough to charge the battery at its peak rate C, the genset is on for exactly $\frac{B}{C}$ time slots in any battery charge-discharge cycle of alternate scheduling. Thus, to estimate the fraction of time the genset is turned off, we only need to calculate the expected number of slots, τ, for which the fully charged battery is discharged. The fuel consumption for the battery-genset hybrid system is then given by

$$k_1 GT \frac{\frac{B}{C}}{\frac{B}{C} + \tau} + k_2 \sum_{t=1}^{T} d(t) \tag{4.7}$$

The life of a storage battery is reasonably well captured by the number of charge-discharge cycles. Suppose w.r.t. fuel cost, one battery charge-discharge cycle costs γ per kWh. We can estimate the monetary expenditure as

$$k_1 GT \frac{\frac{B}{C}}{\frac{B}{C} + \tau} + k_2 \sum_{t=1}^{T} d(t) + \gamma \frac{T}{\frac{B}{C} + \tau} \tag{4.8}$$

Above Eq. 4.7 and Eq. 4.8 allow us to compute the fuel consumption and investment cost of the battery-genset hybrid system for alternate scheduling as a function of the average duration of battery discharge τ. We can get a better intuition of the system's performance by estimating τ using the following assumption.

Assumption: Expected time to discharge a fully charged battery is given by

$$\tau = \frac{B}{E[d(t)]} \tag{4.9}$$

Using the above assumption, we can further simplify Eq. 4.7 to obtain a counter-intuitive result that the fuel consumption is independent of the battery size B.

$$k_1 G T \frac{\frac{B}{C}}{\frac{B}{C} + \frac{B}{E[d(t)]}} + k_2 \sum_{t=1}^{T} d(t) = k_1 G T \frac{\frac{1}{C}}{\frac{1}{C} + \frac{1}{E[d(t)]}} + k_2 \sum_{t=1}^{T} d(t) \qquad (4.10)$$

Note that this does not mean that the system improves genset efficiency even when the battery size is zero. There is an inherent lower bound of $C \leq B$ on the battery size in our discrete time model. If the duration of time slot tends to zero then theoretically both C and B can also tend to zero. However, this would mean that the genset is being turned on and off at an infinite rate, which is practically impossible. Later, in Section 4.5, we numerically verify this intuition.

4.4   Going off-grid

As discussed in Section 4.1, the motivation for this problem is that an industry/ community currently connected to the central grid wants to go off-grid. Thus, historical demand traces are available. The problem is to size both the genset and the battery and schedule power between them such that the total fuel consumption is minimized while ensuring that the loss of load probability is at most ε^*. The battery can help in reducing fuel consumption by both preventing over-sizing of the genset and reducing the running time of the genset. Going off-grid problem is a therefore more general than the Battery-usage problem in Section 4.3.

To avoid over-sizing of the genset, we size the genset smaller than the peak demand and meet rare high demands (a demand greater than G) by using the battery and the genset simultaneously. We note that the loss of load probability can be non-zero as the battery might be empty at a time of high demand. Moreover, loss of load probability is also sensitive to the scheduling as this affects the battery state of charge at the beginning of a high demand. Analyzing battery size, genset size, loss of load probability, and the scheduling simultaneously is difficult. For this section we therefore work with the genset-only scheduling strategy as it gives the minimum loss of load probability. We size the genset and the battery such that the loss of load probability is at most a threshold, ε^*. Any other scheduling strategy, such as the alternate scheduling, might have a higher loss of load probability than ε^*. In Section 4.4.2 we analyze the savings of using a battery to prevent genset over-sizing.

4.4.1 Sizing

For a genset size G, we find a bound on the minimum battery size needed to ensure that the loss of power probability is ε^*. We size the battery for a scheduling that keeps the genset always ON as this gives the minimum loss of power probability, and hence the least battery size. We also assume that the battery charging rate C is 'sufficiently large' and does not affect the least battery size. As we are always in scenario (b) or (c) mentioned in Section 4.2.1, combining the two recurrences we obtain:

$$b(t) = \min\{B, [b(t-1) + \min\{G - d(t), C\}]_+\}$$

We define *deficit battery energy* $b^d(t) := B - b(t)$, which indicates the amount of energy needed at time t to fully charge the battery. We can compute it using the following recurrence:

$$b^d(t) = \min\{B, [b^d(t-1) + \max\{d(t) - G, -C\}]_+\} \tag{4.11}$$
$$= \min\{B, [b^d(t-1) + d(t) - G]_+\} \tag{4.12}$$

where in the last step we use that C is sufficiently large, i.e. $C > \max_t\{G - d(t)\}$.

Using the formulation from Cruz and Liu [13], we solve the recurrence to obtain

$$b^d(t) = \min_{0 \le u \le t-1} \left(\max_{u \le s \le t-1} (D(s,t) - G.(t-s), D(u,t) - G.(t-u) + B) \right) \tag{4.13}$$

As before, we use a concept called statistical sample path envelope. A non-decreasing function $\mathcal{G}$ is a statistical sample path envelope for an arrival process D with bounding function ϵ if it satisfies the following for any $t \ge 0$ and any $\sigma \ge 0$

$$\Pr\{\sup_{0 \le s \le t} \{D(s,t) - \mathcal{G}(t-s)\} > \sigma\} \le \epsilon(\sigma)$$

Using Theorem 1 from [39], we size battery B such that

$$\varepsilon^* = \Pr\{b(t) \le 0\} = \Pr\{b^d(t) \ge B\} \tag{4.14}$$
$$\le \epsilon \left(B - \sup_{0 \le \tau \le t} (\mathcal{G}(\tau) - G\tau) \right) \tag{4.15}$$

Thus, taking $\mathcal{G}(\tau) = G.\tau$, we get
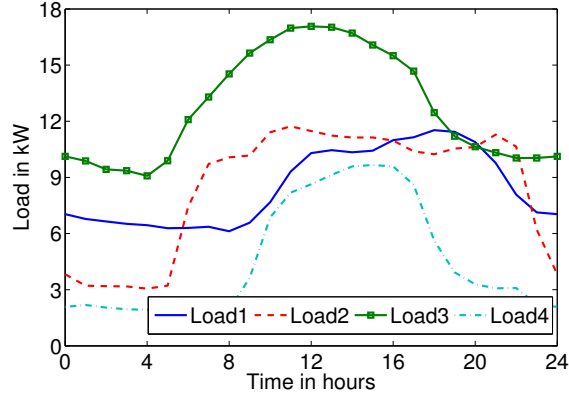
$$B \le \epsilon^{-1}(\varepsilon^*)$$

Figure 4.3: Average typical daily load profile for the four loads

4.4.2 Savings

In this section we estimate the savings in fuel consumption in time $[0, T]$ because of not over-sizing the genset. As loss of load probability is at most ε^*, in absence of battery the genset is sized, $\hat{G}$, to meet at least $1 - \varepsilon^*$ fraction of the total demands, i.e.

$$\hat{G} = \{x : \Pr\{d(t) < x\} = 1 - \varepsilon^*\}$$

Thus, in presence of a battery of size B and genset size G, ratio of new and old fuel consumption is given by

$$\frac{k_1 G T + k_2 \sum_{t=1}^{T} d(t)}{k_1 \hat{G} T + k_2 \sum_{t=1}^{T} d(t)} \tag{4.16}$$

4.5 Evaluation

In this section we numerically evaluate our results for both the battery-usage and the going off-grid problem on an industrial demand data from a local distribution company in Ontario, Canada. The dataset, collected from a local distribution company in Ontario, Canada, contains hourly electricity consumption for four commercial loads for 18 months. We set time slot duration to be 5 minutes and linearly interpolate the demand for the 12 time slots in an hour. Unless otherwise

47

stated, the results are for Load 1 and we set $k_1 = 0.08415$ litre/kW and $k_2 = 0.246$ litre/kWh (i.e. $k_2/k_1 = 2.92$ 1/h) as given in [4]. To compute the offline optimal, we solve the mixed integer program described in Section 4.3.1 using Gurobi Optimizer.

Fig. 4.3 shows the average daily load profile for the four commercial loads. Their mean demands were 8.53kW, 8.59kW, 12.85kW, and 4.70kW respectively. The typical peaking patterns in the graphs is due to variations in activities throughout the day.

4.5.1 Battery-usage

Figure 4.4 and Figure 4.5 helps in making several observations about the savings in fuel consumption using a battery. Firstly, we note that for practical values of parameters k_1 and k_2 carbon footprint is very sensitive to the charging rate. Even for a small charging rate of 2 kW, which is 4 times less than the average load, total fuel consumption reduces by more than 10%. The gains can be more than 20% as the charging rate increases. Secondly, we note that alternate scheduling performs close to the offline optimal. Intuitively, this is true because real demands are stochastic and the worst cases rarely arise. Our worst case example in the proof of Theorem 6 has minimum demands tending to zero followed immediately by maximum demands $G - C$. Such abrupt demand changes that are completely out of synch with the period of alternate scheduling are not common in practice. Thirdly, we see that savings decrease significantly as the value of genset affine function parameter k_2 increases. This is true because a large k_2 in Eq. 4.10 increases the weightage of the term $\sum_{t=1}^{T} d(t)$, which remains unchanged in presence or absence of the battery.

Figure 4.6 helps in evaluating the accuracy of our assumption in Eq. 4.9. We observe that τ is almost a linear function of B and the slope is close to $\frac{1}{E[d(t)]}$. In Figure 4.7, we evaluate our conclusion from Section 4.3.3 that the total fuel consumption for alternate scheduling is not very sensitive to the size of battery. We see that for 5 minute time slots, a battery that can be fully charged in around 30 minutes is sufficient to get the benefits of a battery-genset hybrid system. When we repeated the experiment in Figure 4.7 for smaller values of time slots (figures note shown here), the minimum battery size required to get the benefits decreased further, thus verifying our intuition.

To ensure that this is not the artifact of some specific statistical properties of Load 1, we repeat the example for the other three loads in Figure 4.8. We observe the same behaviour for all the loads.
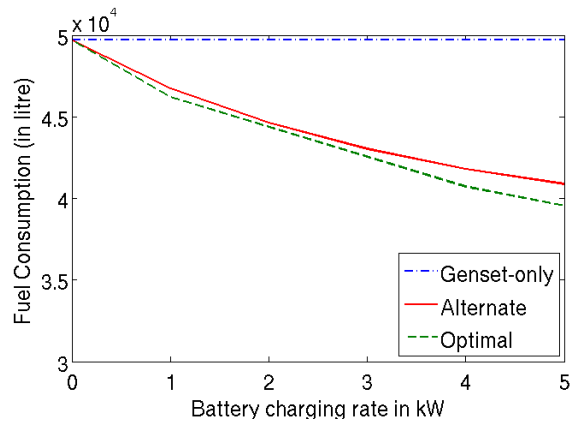
Figure 4.4: **Battery-usage:** Fuel Consumption vs battery charging rate for genset size $G = 25$kW, battery size $B = 3$kWh, $k_1 = 0.08415$ litre/kW, and $k_2 = 0.246$ litre/kWh
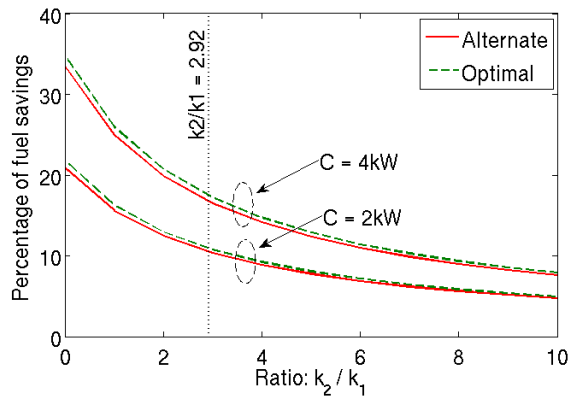

Figure 4.5: **Battery-usage:** Percentage of fuel savings vs ratio k_2/k_1 for $B = 3$kWh
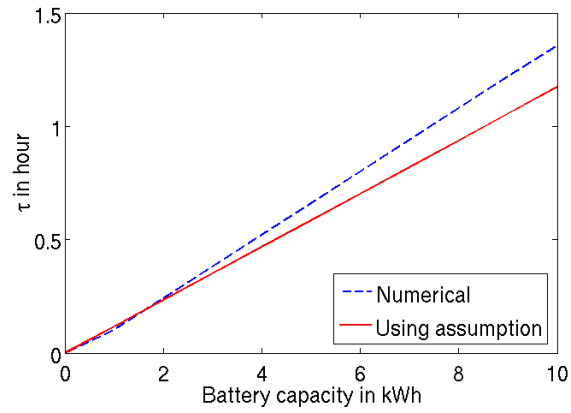
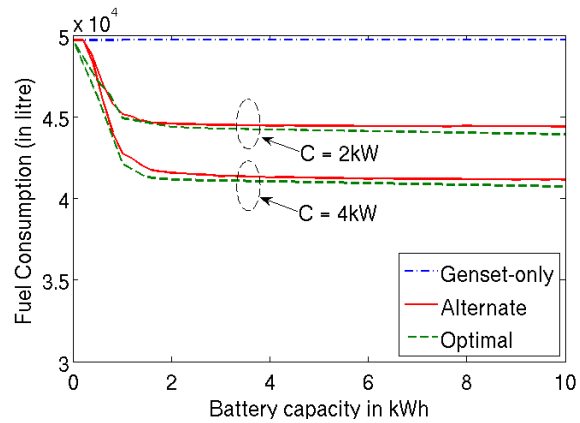Figure 4.6: **Battery-usage:** τ vs battery capacity

Figure 4.7: **Battery-usage:** Fuel consumption vs battery capacity for $k_1 = 0.08415$ litre/kW and $k_2 = 0.246$ litre/kWh
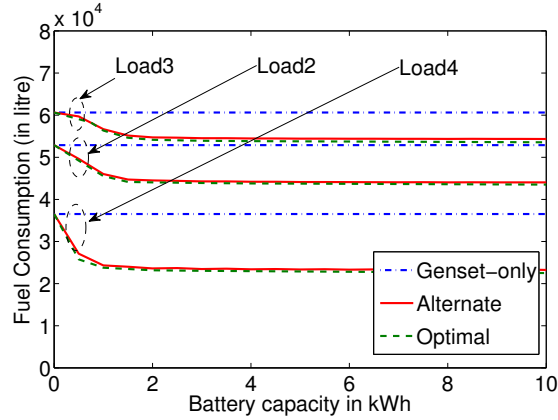
Figure 4.8: **Battery provisioning:** Fuel consumption vs battery capacity. $C = 4\text{kW}$, $k_1 = 0.08415$ litre/kW, and $k_2 = 0.246$ litre/kWh

4.5.2 Going off-grid

In this section we evaluate our sizing formulation from Section 4.4. Figure 4.9 studies the relationship between the genset and battery size while ensuring that the loss of load probability is below a threshold ε^*. We note that the analytical result using statistical sample path envelope is close to the offline optimal. In absence of a battery, the minimum genset size required is less than the maximum demand as the loss of load probability is greater than zero. The dotted vertical lines in the figure show this minimum genset size for $\varepsilon^* = 2.7 \times 10^{-3}$ and $\varepsilon^* = 2.7 \times 10^{-4}$.

Figure 4.10 and Figure 4.11 gives a surprising result that avoiding genset oversizing is not very helpful in reducing fuel consumption. We observe that for the values of parameters k_1 and k_2 given in Reference [4], even a very large battery size of 8kW gives savings of less than 5% in total fuel consumption. This can be attributed to the fact that k_1 is around 3 times less as compared to k_2, which means a large portion of the total fuel consumption, $\sum_{t=1}^{T} d(t)$, remains unaffected (see Eq. 4.16). The savings can be at most 10% if no weightage is given to $\sum_{t=1}^{T} d(t)$.

4.6 Conclusions

Gensets are commonly used today to meet demands at places not connected to the central grid. A battery-genset hybrid system can improve the genset fuel consumption efficiency by meeting
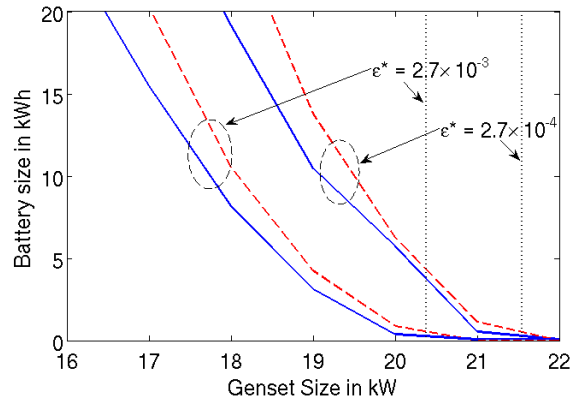
51

Figure 4.9: **Going off-grid:** Battery vs genset size curve. Solid line shows the offline optimal and the dashed line shows the analytical result
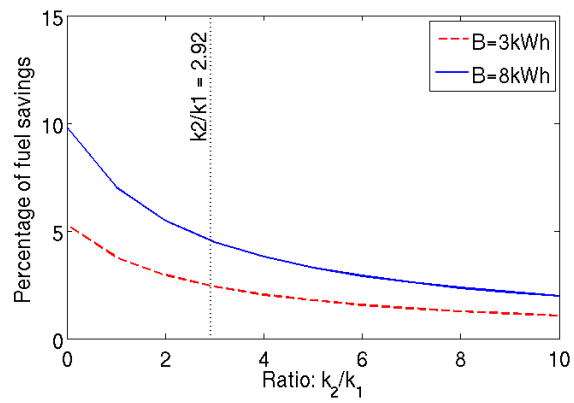

Figure 4.10: **Going off-grid:** Percentage of fuel savings vs ratio k_2/k_1
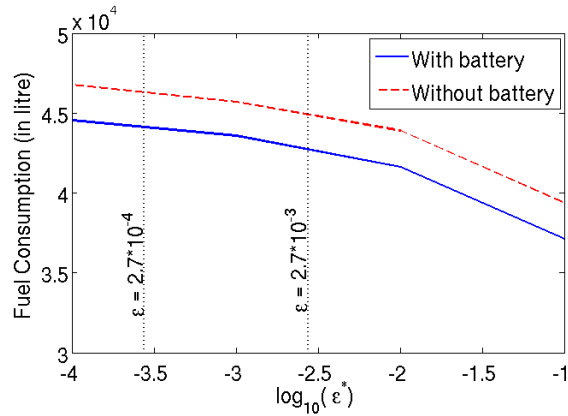
52

Figure 4.11: **Going off-grid:** Fuel consumption vs logarithm of loss of load probability for battery size of 8kWh, $k_1 = 0.08415$ litre/kW, and $k_2 = 0.246$ litre/kWh

low demands entirely from the battery and by preventing genset over-sizing to meet occasional peak demands. We address the problem of scheduling power between genset and the battery to minimize total fuel consumption, and present an online scheduling strategy, alternate scheduling. Using analytical and numerical results we show that alternate scheduling is close to the offline optimal. We give a counter-intuitive result that the total fuel consumption is not very sensitive to the battery size, but is very sensitive to the battery charging rate. Numerically we find that a charging rate of 5kW can reduce fuel consumption by around 20%.

For the general problem of sizing both the genset and the battery, we use analytical technique based on stochastic network calculus to find a bound on the battery size needed to ensure that the loss of load probability is below a threshold ε^*. Numerically, we find that our analytical technique is close to the offline minimum battery size. We also show that using a battery to avoid genset over-sizing can reduce total fuel consumption, however, for practical values of genset fuel consumption parameters this saving is less than 5%.

Chapter 5

Conclusions

Modern society is heavily reliant on electric power. The current power grid is prone to failure, especially in developing countries, either because of unavoidable outages, such as storms, or because of a large gap between demand and supply. In Chapter 3, we investigated the use of storage to allow a set of homes in a single residential neighbourhood to avoid power outages. A storage battery can store power from the grid when it is available and discharge it to meet demand at times of outage. Storage is expensive today and we therefore study the problem of finding the minimum battery size required to ensure that the loss of load probability is at most a threshold ε^*. We use recent results from stochastic network calculus to size storage. Numerical evaluations show that our methodology is within 10% of the minimum battery size required had the future demand been exactly known. Given that diesel gensets are commonly used today to meet demands during a power outage, we also study the problem of using a battery to reduce genset usage, thereby reducing the carbon footprint. Our computation of the carbon emission is within a small factor (1.7) of the value obtained through numerical evaluation.

Many remote locations do not have power grid connectivity and rely completely on diesel gensets to meet their demands. Gensets have greatest energy production to fuel consumption efficiency when they operate close to their capacity. In Chapter 4, we therefore work with a general model of genset where the rate of fuel consumption is an affine, instead of a linear, function of genset power production. We study the two ways of using a storage battery to improve the genset efficiency. Firstly, reducing genset running time by meeting small demands entirely from the battery. Secondly, avoiding genset oversizing by meeting peak demands by simultaneously running the genset and discharging the battery. We give an online scheduling strategy,

alternate scheduling, that has a competitive ratio of $\frac{k_1 \frac{G}{C} + k_2}{k_1 + k_2}$, where G is the genset capacity, C is the battery charging rate, and k_1, k_2 are the affine function constants. We give a counter-intuitive result, both analytically and numerically, that savings in fuel consumption by using a battery is independent of the battery size as long as the battery is sufficient to meet demand for a very few time slots. Numerically we show that alternate scheduling is effective in significantly reducing fuel consumption ($> 10\%$). We also observe that compared to battery-usage, avoiding genset oversizing is not very useful in reducing fuel consumption. Even for large battery sizes, savings in fuel consumption are smaller than 5%.

We realize that the results in this work are limited because of various assumptions. Most of our results have implicitly assumed that the past can give an accurate description of the future. This is not necessarily true as electricity consumption for a particular year might significantly change due to extreme weather conditions. Economic boom or slowdown can also affect industrial demands. One major limitation of our analysis is the battery model. We assume a perfect battery where the battery charging rate C and capacity B are independent. Depending on the technology of the battery, this assumption may or may not be reasonable. An interesting open problem is to extend our results to more complex models of battery where C is a function of B. Moreover, including Peukert's law– the capacity of the battery is a function of rate of discharge– in the battery model would be fascinating.

Our sizing results in Chapter 3 are limited because of lack of demand and outage data from a developing country. Numerical results in Chapter 4, especially that alternate scheduling is close to offline optimal, are for a particular industrial load. Extending them to other industrial loads or finding an analytical argument showing the closeness of alternate and optimal scheduling strategies is an important extension.

Another limitation of our work is that while using the results from stochastic network calculus, we employ a brute force method of finding the leaky bucket and the bounding function parameters to model the stochastic demand. In future work, we hope to find better ways of finding the statistical sample path envelope and the bounding function that do not require this expensive pre-processing step. We also hope to get rid of the statistically independent increments assumption when studying the total loss of power in Chapter 3 and the assumption to estimate expected time, τ, to discharge a fully charged battery in Chapter 4.

References

[1] O. Ardakanian, S. Keshav, and C. Rosenberg. Markovian models for home electricity consumption. In *Proc. ACM SIGCOMM Green Networking Workshop*, 2011.

[2] O. Ardakanian, S. Keshav, and C. Rosenberg. On the use of teletraffic theory in power distribution systems. In *Proceedings of e-Energy*, page 21. ACM, 2012.

[3] O. Ardakanian, C. Rosenberg, and S. Keshav. On the Impact of Storage in Residential Power Distribution Systems. In *Proc. ACM SIGMETRICS Greenmetrics Workshop*, 2012.

[4] P. Arun, R. Banerjee, and S. Bandyopadhyay. Optimum sizing of battery-integrated diesel generator for remote electrification through design-space approach. *Energy*, 33(7):1155–1168, 2008.

[5] J. Boudec and P. Thiran. *A Theory of Deterministic Queuing Systems for the Internet Lecture Notes in Computer Science*. Springer, 2001.

[6] Isidor Buchmann. Charging the lead-acid battery. *Cadex Elec. Inc.* *https://www.classle.net/book/lead-acid-batteries*, Oct 2012.

[7] A. Burchard, J. Liebeherr, and F. Ciucu. On superlinear scaling of network delays. *IEEE/ACM Transactions on Networking (TON)*, 19(4):1043–1056, 2011.

[8] A. Burchard, J. Liebeherr, and S. D. Patek. A Min-Plus Calculus for End-to-End Statistical Service Guarantees. *IEEE Transactions on Information Theory*, 52(9):4105 – 4114, 2006.

[9] CER. Irish Social Science Data Archive. *http://www.ucd.ie/issda/data/commissionforenergyregulation/*, Sept 2012.

[10] C.S. Chang. *Performance guarantees in communication networks*. Springer Verlag, 2000.

[11] F. Ciucu, A. Burchard, and J. Liebeherr. A network service curve approach for the stochastic analysis of networks. In *ACM SIGMETRICS performance evaluation review*, volume 33, pages 279–290. ACM, 2005.

[12] F. Ciucu and J. Schmitt. Perspectives on network calculus: no free lunch, but still good value. In *Proceedings of the ACM SIGCOMM 2012 conference on Applications, technologies, architectures, and protocols for computer communication*, pages 311–322. ACM, 2012.

[13] RL Cruz and H.N. Liu. Single Server Queues with Loss: A Formulation. *Proceedings of CISS 93, Johns Hopkins University*, 1993.

[14] MA Elhadidy and SM Shaahid. Optimal sizing of battery storage for hybrid (wind+ diesel) power systems. *Renewable Energy*, 18(1):77–86, 1999.

[15] A. Elwalid, D. Heyman, TV Lakshman, D. Mitra, and A. Weiss. Fundamental bounds and approximations for ATM multiplexers with applications to video teleconferencing. *Selected Areas in Communications, IEEE Journal on*, 13(6):1004–1016, 1995.

[16] CC Fung, SCY Ho, and CV Nayar. Optimisation of a hybrid energy system using simulated annealing technique. In *TENCON'93. Proceedings. Computer, Communication, Control and Power Engineering. 1993 IEEE Region 10 Conference on*, pages 235–238. IEEE, 1993.

[17] F. Galiana, E. Handschin, and A. Fiechter. Identification of stochastic electric load models from physical data. *Automatic Control, IEEE Transactions on*, 19(6):887–893, 1974.

[18] Y. Ghiassi-Farrokhfal and F. Ciucu. On the impact of finite buffers on per-flow delays in FIFO queues. In *Proc. of ITC*, pages 1 – 8, September 2012.

[19] Jim Iverson. How to size a genset: Proper generator set sizing requires analysis of parameters and loads. *Cummins Power, Technical information*, 2007.

[20] Y. Jiang and Y. Liu. *Stochastic Network Calculus*. Springer Verlag, 2008.

[21] Naazneen Karmali. Powerless In India: 'World's Biggest Blackout' Leaves 600M In The Dark . *Forbes magazine: http://www.forbes.com/sites/naazneenkarmali/2012/07/31/powerless-in-india/*, July 2012.

[22] F. P. Kelly. Notes on Effective Bandwidths. In *Stochastic Networks: Theory and Applications.Royal Statistical Society Lecture Notes Series, 4*, pages 141 – 168. Oxford University Press, 1996.

[23] F.P. Kelly, A.K. Maulloo, and D.K.H. Tan. Rate control for communication networks: shadow prices, proportional fairness and stability. *Journal of the Operational Research society*, 49(3):237–252, 1998.

[24] G. Kesidis and T. Konstantopoulos. Extremal shape-controlled traffic patterns in high-speed networks. *IEEE Transactions on Communications*, 48(5):813 – 819, 2000.

[25] G. Kesidis and T. Konstantopoulos. Extremal shape-controlled traffic patterns in high-speed networks. *Communications, IEEE Transactions on*, 48(5):813–819, 2000.

[26] L. Kleinrock. Queueing Systems. Volume 1: Theory. 1975.

[27] H. Liu. *Buffer Size and Packet Loss in a Tandem Queueing Network*. PhD thesis, UNIVERSITY OF CALIFORNIA, SAN DIEGO, 1993.

[28] A.C. Lloyd and T.A. Cackette. Diesel engines: environmental impact and control. *Journal of the Air & Waste Management Association*, 51(6):809–847, 2001.

[29] S. Mao and S.S. Panwar. A survey of envelope processes and their applications in quality of service provisioning. *IEEE Communications Surveys & Tutorials*, 8(3):2–20, 2006.

[30] Ramya Winstead Mitch Peterson. Definition of effective metrics for evaluating the efficiency of hybrid power systems at telecom cell sites: A system-level approach for determining "tower energy efficiency". *http://cumminspower.com/www/literature/technicalpapers/NAPT-5516-EN.pdf*, Dec 2008.

[31] H.S. Ramakrishna Rahul Tongia, Mohd. Saquib. India Power Supply Position 2010. *Centre for Study of Science, Technology, and Policy CSTEP http://www.cstep.in/docs/India%20power%20supply%20-%20CSTEP%20working%20paper%20No%201.pdf*, Aug 2010.

[32] Michael Graham Richard. Electric Car Battery Prices on Track to Drop 70% by 2015, Says Energy Secretary. *TreeHugger: http://www.treehugger.com/cars/elec*

`tric-car-batteries-track-drop-price-70-2015-says-energy-sec`
`retary.html`, Jan 2012.

[33] EVR Sastry. Village electrification programme in india. In *Photovoltaic Energy Conversion, 2003. Proceedings of 3rd World Conference on*, volume 3, pages 2125–2128. IEEE, 2003.

[34] A.L. Schmid and C.A.A. Hoffmann. Replacing diesel by solar in the Amazon: short-term economic feasibility of PV-diesel hybrid systems. *Energy Policy*, 32(7):881–898, 2004.

[35] Rahul Seth. personal communication, 2012. Sudhir Powering The Nation.

[36] Sloane Simon. Understand Hybrid Generator – Battery Systems: For off-grid applications powered by diesel generators, move to cyclic operation to save costs. Eaton Corporation, White paper, `http://lit.powerware.com/ll_download.asp?file=Understand+Hybrid+Generator+%E2%80%93+Battery+Systems+white+paper_A.pdf`, 2008.

[37] O. Skarstein and K. Uhlen. Design considerations with respect to long-term diesel saving in wind/diesel plants. *Wind engineering*, 13(2):72–87, 1989.

[38] T.H. Sloane, F. Mann, and H. Kaveh. Powering the last mile: an alternative to powering FITL. In *Telecommunications Energy Conference, 1997. INTELEC 97., 19th International*, pages 536–543. IEEE, 1997.

[39] K. Wang, F. Ciucu, C. Lin, and S. H. Low. A Stochastic Power Network Calculus for Integrating Renewable Energy Sources into the Power Grid. *IEEE Journal on Selected Areas in Communications*, 30(6):1037 – 1048, July 2012.

[40] K. Wang, S. Low, and L. Chuang. How stochastic network calculus concepts help green the power grid . In *Proc. of IEEE SmartGridComm*, pages 55 – 60, October 2011.

[41] K. Wu, Y. Jiang, and D. Marinakis. A stochastic calculus for network systems with renewable energy sources. In *Computer Communications Workshops (INFOCOM WKSHPS), 2012 IEEE Conference on*, pages 109–114. IEEE, 2012.

[42] O. Yaron and M. Sidi. Performance and stability of communication networks via robust exponential bounds. *IEEE/ACM Transactions on Networking*, 1(3):372 – 385, June 1993.